The vulnerable coronary plaque: update on imaging technologies

Gian Marco Rosa[1]; Matteo Bauckneht[1]; Giovanni Masoero[1]; François Mach[2]; Alessandra Quercioli[2]; Sara Seitun[3]; Manrico Balbi[1]; Claudio Brunelli[1]; Antonello Parodi[1]; Alessio Nencioni[4]; Nicolas Vuilleumier[5,6]; Fabrizio Montecucco[2,4]

[1]Clinic of Cardiovascular Diseases, Internal Medicine Department, San Martino Hospital and University of Genoa, Genoa, Italy; [2]Division of Cardiology, Department of Internal Medicine, Foundation for Medical researches, University of Geneva, Geneva, Switzerland; [3]Interventional Radiology Department San Martino Hospital, University of Genova, Genoa, Italy; [4]First Medical Clinic, Laboratory of Phagocyte Physiopathology and Inflammation, Department of Internal Medicine, University of Genoa, Genoa, Italy;[5]Division of Laboratory Medicine, Department of Genetics and Laboratory Medicine, Geneva University Hospitals, Switzerland; [6]Department of Human Protein Science, Geneva Faculty of Medicine, Geneva, Switzerland

Summary

Several studies have been carried out on vulnerable plaque as the main culprit for ischaemic cardiac events. Historically, the most important diagnostic technique for studying coronary atherosclerotic disease was to determine the residual luminal diameter by angiographic measurement of the stenosis. However, it has become clear that vulnerable plaque rupture as well as thrombosis, rather than stenosis, triggers most acute ischaemic events and that the quantification of risk based merely on severity of the arterial stenosis is not sufficient. In the last decades, substantial progresses have been made on optimisation of techniques detecting the arterial wall morphology, plaque composition and inflammation. To date, the use of a single technique is not recommended to precisely identify the progression of the atherosclerotic process in human beings. In contrast, the integration of data that can be derived from multiple methods might improve our knowledge about plaque destabilisation. The aim of this narrative review is to update evidence on the accuracy of the currently available non-invasive and invasive imaging techniques in identifying components and morphologic characteristics associated with coronary plaque vulnerability.

Keywords

Vulnerable plaque, atherosclerosis, imaging, nuclear medicine, coronary arteries

Correspondence to:
Fabrizio Montecucco, MD, PhD
Division of Cardiology
Faculty of Medicine, Geneva University Hospital
Avenue de la Roseraie 64, 1211 Geneva 4, Switzerland
Tel.: +41 22 372 71 92, Fax: +41 22 382 72 45
E-mail: fabrizio.montecucco@unige.ch

Financial support:
This research was funded by EU FP7, Grant number 201668, AtheroRemo to Dr. F. Mach. This work was also supported by the Swiss National Science Foundation Grants to Dr. F. Mach (#310030–118245), Dr. N. Vuilleumier (#310030–140736), and to Dr. F. Montecucco (#32003B-134963/1).

Received: February 12, 2013
Accepted after major revision: June 1, 2013
Prepublished online: June 27, 2013

doi:10.1160/TH13-02-0121
Thromb Haemost 2013; 110: 706–722

Introduction

Atherosclerosis is a chronic degenerative dynamic disease of the arterial wall, which mainly involves large and medium-sized systemic arteries. Clinical ischaemic symptoms, such as angina pectoris, usually appear when an increase in myocardial oxygen requirements leads to a transitory imbalance between supply and demand (reduced supply and increased demand). This pathophysiological event is often caused by a coronary plaque that realises a flow-limiting stenosis reducing tissue perfusion (1). If this clinical situation is constant, coronary atherosclerotic plaques have been described as stable lesions of fibrotic morphology (2). Atherosclerosis may, however, take on other clinical forms due to a sudden transition in clinical instability, causing unheralded events, such as myocardial infarction and stroke (3). The transition from asymptomatic (non-obstructive) to symptomatic disease is mainly related to a sudden atherosclerotic plaque rupture and subsequent thrombosis (4). These "vulnerable" lesions might be also non-obstructive plaques (5). Atherosclerotic plaque rupture occurs as a result of the interactions between external mechanical triggers and vulnerable regions of the plaque when forces acting on the plaque exceed its tensile strength (6-8). Even if part of the factors leading to stress on the plaque cap have been identified (i.e. blood pressure, excursion between systolic and diastolic pressure and arterial compliance) and specific intervention have been designed, many of these external forces is still unknown and therefore, it is presently difficult to design effective treatments to prevent plaque rupture. However, plaque tissue properties undoubtedly determine the mechanical strength of plaques and may be a realistic target for therapeutic intervention, thereby decreasing the incidence of heart attack and stroke. Because of the central role of inflammation and hypercoagulability in the genesis and progression of a vulnerable plaque, a variety of circulating biomarkers has been identified (9-11). Although their clinical usefulness in the early diagnosis of acute myocardial infarction (AMI) has not been demonstrated yet, the measurement of inflammatory biomarkers of plaque vulner-

ability (such as myeloperoxidase [MPO], C-reactive protein [CRP], interleukin [IL]-6), or CX3CL1/fractalkine) and of blood markers reflecting thrombogenic activity (fibrinogen, D-dimer, soluble (s)CD40L, sP-selectin and activated platelets) could provide some incremental information regarding the risk stratification of patients (12-14). Despite the potential use of systemic biomarkers, the identification of the anatomic localisation of the plaque remains missing. Therefore, we believe that anatomically precise imaging is a medical need.

The "vulnerable plaque" was firstly defined as a non-obstructive, silent coronary lesion that suddenly becomes obstructive and symptomatic (15). It is responsible for the majority of acute coronary events (16). The most complete definition of this phenomenon was proposed in 2003 by Naghavi et al. (15), reporting that vulnerable plaques are not only susceptible to rupture, but they are more broadly susceptible to thrombosis or may rapidly progress to a culprit lesion. On the basis of large retrospective autopsy studies (17-19), major and minor functional criteria were defined to potentially assess the degree of vulnerability of a plaque (15) (►Table 1). Some atherosclerotic plaque features are particularly associated to vulnerability: structural characteristics (increased lipid content, between 10 and 25%, the presence of a thin cap [<65 μm]), inflammatory cellular accumulation (activated macrophages), presence of positive remodelling of the coronary vessel and neovascularisation. The size of the necrotic core and the thickness of the fibrous have been indicated as major structural determinants of vulnerability (20, 21). These aspects make the cap of a plaque less resistant to the circumferential wall stress (22-24). The composition of the lipid necrotic core of a vulnerable plaque is characterised by an increased free/esterified cholesterol ratio, resulting in a higher risk of rupture and thrombosis (24-26). The high lipid content could be the reason for the yellow color of this type of plaque (15). Inflammatory cell infiltration a vulnerable plaque is particularly capable of degrading the extracellular matrix by secretion of proteolytic enzymes (27, 28). Their activation is also related to a higher risk of intraplaque haemorrhage (IPH) (29) that is one of pivotal event in plaque disruption. As shown in a rabbit model (30), the accumulation of erythrocyte membranes within the lesion may increase the risk of plaque destabilisation by contributing to the deposition of free cholesterol, macrophage infiltration, and enlargement of the necrotic core (31). Another possible mechanism is that when a red blood cell (RBC) is damaged it releases its iron content which can activate the reactive oxygen species (ROS) thereby increasing the plaque vulnerability for rupture (30, 32). A vulnerable plaque has been shown to stimulate a vessel's compensatory remodelling due to the digestion of the internal elastic lamina, which results in an eccentric growth of the atheroma and an outward enlargement of the vessel wall without luminal compromise (15, 33-35). Historically, the most important diagnostic technique for studying atherosclerotic disease was to determine the residual luminal diameter by angiographic measurement of the stenosis. However, it has become clear that vulnerable plaque rupture as well as thrombosis, rather than stenosis, triggers most acute ischaemic events and that the quantification of risk based merely on severity of the arterial stenosis is not sufficient. Therefore, in the last few decades a great deal of progress has been made in the field of techniques that allow us to study arterial wall morphology, plaque composition and its inflammation, and metabolic processes. Despite some limitations due to the fact that a "histologically" defined vulnerable plaque might not clinically rupture (36), a gold-standard imaging technique should check each one of these structural characteristics to identify a vulnerable plaque. This technology should have high resolution in order to measure the cap's thickness. It should also allow identifying and quantifying the cap's cholesterol and the composition of the inflammatory cells, the presence of IPH, the iron content and the positive vessel remodelling. Since the composition of the high-risk plaques varies, depending on their anatomical size, with striking heterogeneity even within the same individual (37), non-invasive imaging modalities that are able to detect and characterise atherothrombotic lesions in their various stages and their different anatomical regions are clinically needed. Non-invasive techniques might allow us to rapidly screen low-moderate risk patients and therefore to prevent acute coronary syndrome (ACS). On the other hand, invasive techniques that have high microscopic resolution are needed to study the plaque composition during angiography in patients with known atherosclerotic disease.

The aim of this narrative review is to update evidence on the accuracy of the currently available non-invasive and invasive imaging techniques in identifying the plaque components and morphologic characteristics associated with plaque vulnerability that could be used to improve the risk estimation of acute coronary events. This review of the published literature is based on the material searched for and obtained via MEDLINE, PubMed and EMBASE up to November 2012. The search terms we used are: "atherosclerosis, plaque, vulnerability, instability, rupture risk" in combination with: "imaging, ultrasound, intracoronary imaging, IVUS, CT, MRI, PET, SPECT, nuclear medicine".

Non-invasive techniques

Computed tomography (CT)

The possibility to non-invasively visualise coronary anatomy is the main reason for the current interest in CT. Its high temporal and spatial resolution allows detailed anatomical delineation of large

Table 1: Histological criteria of plaque vulnerabilty. The presence of at least one of the major criteria or more than one minor criterion may indicate a higher risk for plaque complication. Adapted from Naghavi et al. 2003 [9, 15].

Major criteria	Minor criteria
Thin cap (< 100 μm) with large lipid core (>50% of the plaque's total volume)	Superficial calcified nodule
Active inflammation	Yellow colour of the plaque
Endothelial denudation or superficial platelet aggregation	Intraplaque haemorrhage (IPH)
Stenosis (>90%)	Endothelial dysfunction

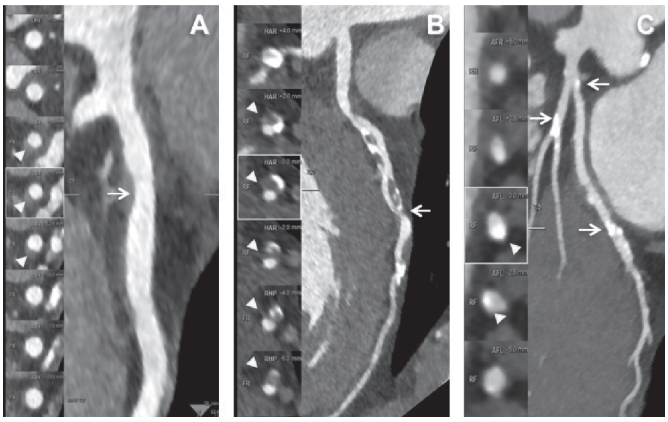

Figure 1: CT images of non-calcified plaque, mixed plaque, multiple spotty calcified plaques. A) Example of non-calcified plaques with corresponding transversal sections. MDCT curved multiplanar reconstruction of the left anterior descending artery (LAD) showed a non-calcified plaque associated with positive remodelling and non-significant obstruction of the lumen (<50%) in the proximal segment (arrow). MDCT axial images (arrowheads) display short axis views at the site of the coronary lesion. The median (interquartile range) of MDCT densities of the plaque was 27 (20-60) HU. B) Example of mixed plaque with corresponding transversal sections on the left. MDCT curved multi-planar reconstruction of LAD showed extensive mixed-type atherosclerotic disease with positive remodelling involving the proximal and medium segment of LAD, associated with significant (>50%) obstruction of the lumen (arrow). MDCT axial images display short axis views at the site of the coronary lesion (arrowheads). The median (interquartile range) of MDCT densities of the plaque at this level was 226 (158-583) HU. C) Example of multiple spotty calcified plaques of left circumflex artery (LCX) and LAD (arrows). Cross sectional views perpendicular to the axis of mid segment of the LAD showed calcified plaques without significant luminal obstruction (arrowheads). Note the artifact of "blooming" due to partial volume averaging of dense calcium (which typically has an elevated atomic number). The median (interquartile range) of MDCT densities of the plaques at this level was 771 (753-863) HU.

and medium-sized vessels, so this technique can be considered the most accurate clinical method for non-invasive coronary angiography. In 2000, 4-slice CT systems allowed coronary artery imaging for the first time, but only the proximal parts of the coronary artery were interpretable because limited spatial and temporal resolution restricted their clinical value for coronary artery visualisation (38). With the introduction of 16- and 64-slice systems, improved temporal and spatial resolution, as well as substantially shorter scan times led to improved image quality throughout the entire coronary tree (39). A meta-analysis conducted in 2007 by Vanhoenacker et al. demonstrated a significant improvement in the accuracy for the detection of coronary artery stenosis for 64-slice CT when compared with previous scanner generations. The pooled sensitivity and specificity for detecting a greater than 50% stenosis per segment were 93% and 96% for 64-slice CT, 83% and 96% for 16-slice CT, 84% and 93% for 4-slice CT, respectively (40). In addition, a 256-slice CT system, whose large coverage along the patient's longitudinal axis may allow for imaging of the entire heart in a single cardiac cycle, will become available in the near future (41). The consistently high negative predictive value of CT angiography suggests that this exam should be recommended to rule out coronary stenoses (42). It may be also used to visualise earlier stages of coronary atherosclerosis. Coronary calcium, a surrogate marker for the presence and amount of coronary atherosclerotic plaque, can be detected and quantified by non-contrast CT, allowing us to stratify asymptomatic individuals with a stronger predictive power than stratification based on traditional risk factors (43). Coronary calcium measurements by CT may be useful in patients who, based on prior assessment of standard risk factors, seem to be at intermediate risk for future coronary artery disease (CAD) events. It may also be valuable when deciding to start lipid lowering therapy. Inoue et al. (44) evaluated the plaque changes (plaque, low attenuation plaque and lumen volume, remodelling index) by serial coronary CT angiographies in 26 statin-treated patients as compared to eight subjects who refused the statin treatment (controls). Serial CT angiographic evaluations of coronary plaques allowed for the assessment of statin treatment-related reduction of the plaque and necrotic core volume. Although larger clinical studies are needed, a CT preliminary assessment of the plaque composition might be useful to evaluate anti-atherosclerotic effects of statin treatment.

The high CT attenuation of calcified structures allows for a simple visual and qualitative characterisation of plaque composition by dividing coronary lesions into calcified, non-calcified and mixed plaques (►Figure 1). Surprisingly, a higher prevalence of non-calcified and mixed plaques was found in the culprit lesions of patients with ACS, while patients with stable angina had more commonly calcified lesions. This evidence suggests that diffuse intraplaque calcification might be not associated with vulnerability.

The culprit lesions of patients with AMI, unstable angina and stable angina have been shown to have different calcification patterns. In particular, in patients with AMI spotty calcified deposits within an arc of ≤90° were found (45). On the basis of the good correlation between intravascular ultrasound (IVUS) and multidetection CT (MDCT) in the evaluation of coronary plaques, and particularly the excellent sensitivity of MDCT in differentiating calcified and soft components, MDCT can be considered as a promising non-invasive standard criterion to accompany the invasive imaging modalities (43).

IVUS defined thin-cap fibroatheromas (TCFAs) in ACS patients are more frequently associated with lesions classified as mixed by CT angiography (CTA) (46). With regard to non-calcified plaques, there is a lack of persuasive evidence suggesting a reliable sub-classification of plaques as lipid-rich vs fibrous based on CT density measurement (47). The large plaque and necrotic core volumes in vulnerable plaques, as well as the outward vascular remodelling are identifiable by CTA. Density based software has been used to automatically define the plaque territory around the luminal contrast and to identify the necrotic cores. The culprit lesions in patients presenting with acute coronary events are positively remodelled, enclose a large soft area (less than 30 Hounsfield units), and reveal spotty calcium deposits.

The substantial difference in the mean density of these plaques is not only related to the lipid component, but is linked to the micro-architecture composition of the plaque itself which in addi-

tion to triglycerides is also composed of cholesterol, necrotic material, smooth muscle cells and microscopic calcified components (48, 49).

The absence of vascular remodelling, of large soft area and of spotty calcium deposits in culprit lesions has never been reported in a patient with an acute coronary event; while on the other hand, the presence of all three characteristics in a plaque corresponded to a 95% likelihood of the lesion being a culprit lesion (50). In a prospective study of more than 1,000 patients, the same investigators reported positively remodelled soft plaques in 7% of patients, and up to one-quarter of these individuals sustained an acute coronary event within the 48 month follow-up period. Conversely, patients who did not have these features in their plaque demonstrated less than 0.5% likelihood of developing an acute event over the same follow-up period. This study also confirmed that the plaques that were subsequently involved in acute events typically had a greater necrotic core volume and demonstrated positive remodelling in the initial CT angiography compared with plaques that were not implicated in acute coronary events (51).

Considering that current CTA devices do not reach enough spatial resolution to detect the thickness of the fibrous cap, this technology is unable to investigate this structure within plaques (52). Recently, a new sign of plaque vulnerability has been proposed: a contrast rim around the plaque described as a ring-like contrast enhancement surrounding the coronary lesion. This imaging phenomenon may reflects vasa vasorum (VV) neovascularisation of the plaque with active inflammation ring; other possible explanations are the presence of contrast surrounding thrombus material or of a large necrotic core separated by fibrous contents or native vessel wall (53, 54). This sign, although insensitive, was shown to be the strongest MDCT feature associated with TCFA at the culprit site, with a reported specificity >95% (53, 55).

Future developments (other than increased spatial and temporal resolution) are going to improve detection of vulnerable plaques by MDCT, such as the use of multiple energy data sets (80 kV and 140 kV), reducing the overlap of the attenuation of plaque components, and improving the possibility to highlight histological findings potentially related to clinical vulnerability. CT has also shown promising preliminary results in the context of molecular imaging of intraplaque inflammation using targeted nanoparticle contrast agents. For example, N1177, a suspension composed of crystalline iodinated particles dispersed with surfactant with a high affinity to activated macrophages is used (56). In atherosclerotic rabbits, CT density of plaques after N1177 injection correlated with FDG uptake (57). However, despite encouraging findings in animals, some authors have raised concerns about the low sensitivity of CT at detecting molecular contrast agents (58). Spectral (or multi-colour) CT, which can identify types of tissue based on their characteristic energy-dependent photon attenuation, may thereby enhance the sensitivity of CT to detect targeted contrast agents. In atherosclerotic mice, spectral CT enabled the detection of intraplaque inflammation after injection of gold-labelled high-density lipoprotein (HDL) nanoparticles designed to target activated macrophages (59). The feasibility and clinical applicability of CT for molecular imaging of plaque vulnerability awaits clinical translation to humans.

Magnetic resonance imaging (MRI)

MRI is a non-invasive imaging technique, which can offer an early assessment of the overall extent of carotid atherosclerotic burden in symptomatic patients, and the characterisation of the so-called "vulnerable" high-risk plaques. The patient is placed in a strong magnetic field, and images are obtained on the radiofrequency signal from water protons following administration of a radiofrequency pulse. The emitted signal varies according to the water concentration and the relaxation times: T1 and T2. By using T1-weighted, T2-weighted and proton density-weighted imaging it is possible to determine plaque anatomy and composition. Multiple MR-sequences, either with bright-blood (time of flight TOF) and black-blood flow suppression may help to identify the main components of vascular lesions such as the fibrous cap, lipid-rich necrotic core (LRNC), IPH, neovasculature and signs of vascular wall inflammation (60, 61).

Different studies have demonstrated that *in vivo* multicontrast magnetic resonance of human carotid arteries has a sensitivity of 85% and a specificity of 92% for the identification of a lipid core and IPH (62, 63). Other extensive MRI studies have validated the characterisation of plaques by histological analysis of retrieved carotid endarterectomy specimens. In patients with mild to moderate stenosis, the thin/ruptured fibrous cap was found to be associated with a lipid-rich necrotic core and symptoms, whereas in patients with severe stenosis, only the presence of ulceration at MR was associated with symptoms (64). Among the 138 patients who had moderate-severe carotid stenosis of 50-79%, the ones whose plaques were characterised by thinned or ruptured fibrous cap, large lipid necrotic core, IPH and maximum wall thickness had a higher incidence of cerebrovascular accidents (65). Thus, emerging evidence potentially links the biomechanical forces to the pathogenesis of plaque vulnerability and to the timing of symptoms. Using MRI to calculate the mechanical stress with carotid plaques, Sadat et al. suggested that the maximum circumferential stress within the plaques of patients with acute symptoms exceeds that in plaques of recently symptomatic patients and that plaques associated with recurrent transient ischaemic attack (TIA) have significantly higher stress than those associated with a single episode of TIA (66). As far as IPH is concerned, this may be visualised owing to the fact that the degradation of haemoglobin to metahaemoglobin shortens the relaxation T1 times. Furthermore, recent haemorrhage appears as a bright signal on black-blood T1-weighted sequences and magnetisation-prepared rapid acquisition gradient echo (MP-RAGE) (67). Some MR studies have suggested a role for IPH in plaque destabilisation and have underlined its connection with subsequent cerebrovascular events. This role was questioned by Zhao et al. recently in a study of 181 patients (68-70). IPH contributes to two features that synergistically increase the odds of plaque rupture: necrotic core size and plaque volume (71). The accurate identification of IPH in patients with symptomatic carotid

diseases may be improved with the use of T1-weighted turbo spin echo sequences (TSE) (72, 73).

Since Sullivan first proposed that relative iron depletion was protective against cardiovascular disease, research has focused on the role of iron in atherosclerosis (74). Micro-haemorrhage with macrophage-mediated phagocytosis and degradation of aged red blood cells in atherosclerotic plaques leads to an accumulation of redox-active iron. Iron catalyses the degeneration of oxidised low-density lipoprotein (LDL) via Fenton chemistry, and this accelerates atherosclerosis. By using non-invasive carotid plaque T2 measurements, Raman et al. found characteristic changes in various forms of iron (decreased levels of paramagnetic-FE-(III) complexes and similar total iron levels) in plaques that cause symptoms, thus supporting the dynamic presence of iron in the microenvironment of atherosclerotic plaques (75).

On the other hand, while well-validated sequences and dedicated coils are available for obtaining images of the carotid arteries and "vulnerable" plaques by MRI, cardiac and respiratory motion limits the current effectiveness of imaging in the coronary tree. Due to the presence of issues related to resolution, i.e. partial volume loss and low signal to noise ratio (SNR), the use of multi-contrast MRI is limited to large arteries such as the carotid arteries or aorta. Therefore, due to motion, size and structure of the vessels, imaging of the coronary arteries remains challenging with multi-contrast MRI techniques (76). Contrast agents are needed to further improve the detection and characterisation of vulnerable plaques by MRI. Recent studies with nonspecific contrast agents have shown that these agents improve the detection and characterisation of plaque components. Gadolinium, a contrast agent, is able to spread throughout the pathologic endothelium or the neovasculature in atherosclerotic plaque. Gadolinium enhancement occurs in the fibrous cap and may correlate with the neovascularisation. Thus, the use of these agents increases accuracy in identifying various plaque structures indicative of vulnerability (necrotic lipid core, fibrous cap and neovasculature [77, 78]). Molecular imaging is challenging for the detection of vulnerable plaques owing to the fact that molecular targets are often present in very small numbers, so molecular imaging probes need to be designed. As far as plaque vulnerability is concerned, active intraplaque macrophages are one of the earliest MR targets that were studied. Oxidised LDL, extracellular matrix, thrombus and receptors associated with neovasculature are other targets indicative of plaque vulnerability (79). As stated earlier, the activation of mononuclear phagocytes promotes the evolution of the atherosclerotic lesion. MRI may help to identify macrophage accumulation in the atherosclerotic plaque by examining dynamic kinetics of tissue enhancement after administering gadolinium contrast (80, 81) and by utilising USPIOS that target macrophages *in vitro*. Enhancement of plaque tissue with Gadolinium contrast correlates strongly with macrophage content. Furthermore, activated macrophages infiltrating the plaque internalise ferromagnetic USPIOS, and this leads to a change in the resonance frequency of surrounding water molecules and to a shortening of their relaxation times that appears with signal loss in T2-weighted sequences (82). Various studies on carotid arteries have demonstrated the effects of statins on the progression of atherosclerotic plaque. Carotid MRI may be considered an ideal technique for monitoring vessel wall changes under treatment, and it has been extensively validated for its ability to evaluate plaque regression (83, 84). In the Familial atherosclerosis treatment study (FATS), carotid MRI demonstrated that prolonged intensive lipid lowering therapy is associated with a decreased lipid content of the atherosclerotic plaque, a characteristic of clinically stable plaque (85). Orion trial MRI showed that long-term treatment with rosuvastatin was associated with a reduction of the lipid-rich necrotic core, whereas the overall plaque burden remained unchanged (86). The ATHEROMA TRIAL used USPIOS in 40 patients to demonstrate that aggressive lipid-lowering therapy with atorvastatin over a three-month period is associated with a significant reduction in plaque-uptake (87). As a result, MRI represents a promising technology for imaging vulnerable plaques thanks to the absence of ionising radiation, even if its application is limited to large arteries such as carotid arteries or the aorta due to its spatial resolution. Imaging of the coronary arteries remains challenging due to the limited temporal resolution that hampers its application in the coronary circulation. The main advantages of this technique are that it is non-invasive and may be repeated sequentially over time.

Nuclear imaging

The rationale for the use of nuclear techniques in atherosclerosis imaging is that, thanks to its emission of gamma rays, a radiotracer can be co-localised with a cell or receptor of interest in the plaque, thus showing its functional characteristics. Those characteristics can be applied to non-invasively detect inflamed and potentially rupture-prone lesions.

The main advantage of nuclear imaging is its excellent sensitivity which allows us to detect sparse targets in the nanomolar range using a low tracer dose. Even though single photon emission computed tomography (SPECT) and positron emission tomography (PET) were historically burdened by the low spatial resolution, hybrid imaging techniques have recently been introduced, adding the information of a molecular signal to the anatomical data obtained by CT and MRI. This progress has led to an increase in interest in the application of these techniques to the cardiovascular system.

PET

In 2001, for the first time, fluorine-18-fluorodeoxyglucose (FDG) uptake was accidentally found in the vascular wall of large arteries in a patient being studied by PET for cancer (88). The following year Rudd et al. (89) demonstrated the uptake of this radiotracer in human carotid plaques associated with ischaemic stroke. These data were confirmed by other studies which showed that FDG is taken up by macrophages and other hyper-metabolic cells within plaques where it can be measured by PET imaging, thus providing an opportunity for non-invasive functional imaging of atherosclerosis and showing that the greater the plaque inflammation, the greater the FDG uptake (90, 91). In control patients, not only

did culprit lesions have a greater concentration of inflammatory cells than normal arteries but also in comparison with stable plaques (92). Following these findings, several clinical trials used FDG uptake as a marker of inflammation within plaques and some of these trials revealed that treating patients with simvastatin resulted in a significant reduction in carotid plaque inflammation and consequent FDG uptake compared to dietary management alone, having also a pharmacological impact (93).

FDG-PET has also been used to define coronary plaques by prescribing a high-fat/low-carbohydrate diet in order to reduce the myocardium glucose uptake before the exam (94). An early pilot study conducted on coronary arteries demonstrated that FDG coronary uptake is often associated with symptoms of acute myocardial ischaemia (95).

Despite these advantages, some issues must be solved before embracing FDG-PET as an elective imaging technique in the field of coronary vulnerable plaque. First of all, only limited prospective data show that FDG uptake or changes in FDG uptake are correlated to cardiovascular events (96), so it is necessary to wait for results of larger prospective cohort studies. Data on FDG uptake lack standardisation and data concerning false positive/negative sensitivity and reproducibility are still rudimentary (97). In addition, although coronary plaque imaging is feasible with FDG-PET/CT, this approach seems not qualified for the detection of histological features of plaque vulnerability. In fact, inflammatory activity in vulnerable plaques has been shown to play a pivotal role when located in the very tiny regions of the fibrous cap. However, FDG activity detected by the whole-body PET/CT is unlikely to measure specific macrophage activity around the fibrous cap. PET/CT rather assesses the whole plaque inflammatory activity. The last challenge that needs to be overcome is that mechanisms (other than inflammation, such as hypoxia) may generate the FDG uptake signal associated with the plaque. Therefore, even if FDG seems to be a good marker of inflammatory atherosclerotic plaques, it cannot presently be used as a predictor of outcome of a given coronorary atherosclerotic lesion.

The limitations of FDG-PET in vulnerable plaque imaging require us to focus on novel detectable markers of the plaque biology. In fact, depending on the radiotracer, a wide variety of physiological and pathological processes can be studied at the molecular level using PET. In 2006, Matter et al. observed a choline accumulation in the macrophages of activated atherosclerotic plaque in a murine model using Fluorine-18-labelled fluorocholine (18F-FCH) PET imaging (98). This technique allowed for better identification of plaques as compared to FDG-PET. In 2008, for the first time, Bacerius et al. (99) described the use of this radiotracer in human abdominal aorta and common iliac arteries. Fluorine-18-labelled fluoromethylcholine (18F-FMCH) showed promising results in detecting non-calcified lesions of the vessel wall, both in solely structural wall artery and in combined lesions with structural wall artery and inherent calcified parts. On the other hand, solely calcified vessel lesions did not uptake the tracer at all. Another prospective study has been carried out recently in this field (100), analysing the 18F-NaF uptake in the coronary arteries by PET/CT. In this study, Dweck et al. stated that coronary uptake of 18F-NaF reflects active calcification in the atherosclerotic plaque, offering additional and complementary information to the CAC scoring detected by CT. Several prospective studies are now needed to determine the relationship between 18F-NaF uptake, morphological plaque characteristics and future cardiovascular events, and to identify novel detectable markers.

All these studies are limited not only by the appropriateness of the radiotracer, but also by the small size of the region of interest for target localisation in a beating heart, and the difficult preparation of the patient (94).

SPECT

SPECT differs from PET in several ways, including spatial resolution and imaging sensitivity (▶Table 2). In addition, specific SPECT ligands have been tested for probing some pathophysiological processes of atherogenesis such as apoptosis, lipoprotein accumulation, inflammation, chemotaxis, angiogenesis, proteolysis, and thrombogenicity (101).

Apoptosis of smooth muscle cells and macrophages is an important indicator of atherosclerotic plaque vulnerability. Annexin A5 is a protein which targets the phosphatidylserine surface expression of cells during the apoptotic process. Based on animal studies (102-104), the technetium Tc-99m-labelled annexin A5 detection has been proposed to humans as a non-invasive *in vivo* technique to detect unstable atherosclerotic lesions. The first study in this field, reported by Kietselaer et al. (105), analysed the Tc-99m-labelled annexin A5 uptake in carotid atherosclerotic plaques of four patients with frequent TIA. They demonstrated that SPECT apoptosis detection of culprit lesions before endarterectomy correlated with post-operative histological findings. Other human studies have been conducted, and have also shown the impact of statin therapy on the reduction of plaque apoptosis. A significant reduction in Tc-99m annexin A5 uptake after dietary modification and simvastatin therapy was observed by Hartung et al. (106). Despite these promising results, the use of Tc-99m-labelled annexin A5 to detect apoptosis is limited (107) because of a lack of resolution and specificity due to the tendency of annexin A5 to bind phosphatidylserine expressed by platelets within the thrombus, in addition to imaging difficulties of the coronary tree such as small plaque size and cardio-respiratory motion. Furthermore, this radiotracer is not yet commercially available for clinical use (108). Further development of this tracer may eventually help to solve this preclinically observed difficulty to reach the clinical domain. Although 99mTc-annexin A5 remains the most

Table 2: Differences between PET and SPECT notable for atherosclerotic plaque imaging. Adapted from: Nahrendorf M, et al. [221].

	PET	SPECT
Spatial resolution (mm)	1–2	0.3–1
Imaging sensitivity (mol/l)	10(-11)-10(-12)	10(-10)-10(-11)
Depth of penetration	no limit	no limit

largely studied tracer of apoptosis, alternative peptidic and non-peptidic agents have been described, but the behaviour of these new compounds warrants further investigation.

In order to study atheromatous plaques, LDL has been labelled with several radioisotopes such as: Iodine-123, Indium-111 and Tc-99m (109). Among them, Tc-99m showed the greatest sensitivity for detecting vulnerable lesions, overall when labelled to oxidised LDL (110). Lectin-like oxidised LDL receptor 1 (LOX-1) is a cell surface receptor for oxidised LDL that has been implicated in vascular cell dysfunction related to plaque instability. In 2008, Ishino et al. (111) designed and prepared 99mTc-labelled anti–LOX-1 monoclonal IgG and investigated its usefulness as an atherosclerosis imaging agent. The accumulation ratios of 99mTc-LOX-1-mAb for validated lesion ratios (such as atheromatous/neointimal, atheromatous/fibroatheromatous, and atheromatous/collagen-rich) were higher than those of 99mTc-annexin A5. These results suggest that LOX-1 might be promising to identify vulnerable plaques. This observation was confirmed by Li et al. (112), but further experimental studies are still needed for the validation of this compound. Another way to characterise a vulnerable plaque could be to detect peptides associated with LDL. Hardoff et al. (113) showed a significant uptake of a radiotracer based on the apo-B portion of LDL. Their experiment obtained weak results and to date, there are no noteworthy published studies applied to man.

Although several studies have attempted to show a correlation between plaque morphology and the measurement of macrophage content by detecting the antibodies directed at these cells, none of them were successful (113-117). One of the most recently proposed techniques for quantifying the inflammatory cell content of a plaque is to visualise the expression of chemokines or receptors within the vascular wall. Monocyte chemoattractant protein-1 (MCP-1) is one of the strongest chemotactic agents, attracting inflammatory cells to the atherosclerotic lesion. Ohtsuki et al. localised its receptor using 125I-MCP-1 in atheroma of rabbits (118). 125I-MCP-1 activity correlated with macrophage content per unit area as confirmed by successive *ex vivo* immunohistochemistry and autoradiography results. Furthermore, elevated circulating MCP-1 levels have been found in patients with CAD and have been correlated with disease progression and poor prognosis (119). These data make this radiotracer interesting, thus further investigations are needed to show its potential in humans.

Matrix metalloproteinases (MMPs) are enzymes that degrade extracellular matrix components which play a crucial role in plaque rupture (120, 121). Understanding the precise activity of MMPs within the promotion of plaque destabilisation could be of great help in the field of preventing cardiovascular events. Furthermore, Xie et al. demonstrated the potential benefit on plaque stability of therapeutically inhibiting MMP activity (122). Several studies have been conducted to analyse the feasibility of SPECT imaging of MMPs, most of them on animals, using Tc 99m as the radiotracer (123-126). Recently, Razavian et al. proposed the use of micro-SPECT and a radiotracer that specifically targets the MMP activation epitope to evaluate MMP activity in mice under high-fat diet (127). The most relevant observation of this study is the *in vivo* heterogeneous uptake of tracer along the aorta of mice, demonstrating a correlation between MMP content and plaque activity. Although the detection of MMPs by SPECT is very appealing, further studies are needed to demonstrate the diagnostic accuracy in the detection of rupture-prone plaques as well as to investigate the risk-benefit ratio (128). Wagner et al. recently described the first synthesis of an 18F-labelled MMP inhibitor usable in man (129). The first results of this human application should be available in the near future.

Limitations to the clinical application of non-invasive imaging techniques

A future challenge is the translation of these preliminary results from animals to human beings. First of all, it is necessary to determine which modality is most suitable for near-term clinical application and which possesses the tools required to highlight a plaque in a quickly moving, narrow artery such as the coronary artery (2.5–3.5 mm diameter). A second problem is represented by the cost-effectiveness ratio. Nuclear imaging will not likely become a routine clinical application as a screening tool for vulnerable plaques in unselected populations in the near future, but it could become part of a tiered management strategy that first stratifies the risk population, and then is only applied to high-risk subpopulations (130). However, one application for these technologies could be to find early signals of drug efficacy and to identify the correct doses, thereby minimising side effects.

Invasive techniques

Intravascular ultrasound (IVUS) on the vulnerable plaque

IVUS technology was invented in 1972 (131). An ultrasound unit is mounted on the tip of a catheter. This unit can consist of a single element piezoelectric material with a frequency range between 30 and 45 MHz or of an array of 64 elements with a center frequency of 20 MHz (132). With regard to single element catheters, the beam will be steered by mechanically rotating the element, while for the array, the beam will be steered electronically (133). Rotation devices are able to produce an image with a resolution between 100 and 150 μm (134). Phased array catheters are generally easier to set up and more flexible, but historically have suffered from lower resolution when compared to their mechanical counterparts, and this may result in poorer near field imaging (135). These catheters can be advanced through the groin, then through the aorta all the way into the coronary arteries, thus a tomographic image of the vessel, vessel wall and atherosclerosis can be created (133).

In the normal artery, two interfaces are usually observed, one at the border between blood and the leading edge of the intima and a second at the external elastic membrane (EEM), which is located at the media adventitia border. The tunica media is relatively sonolucent and, in good quality images, it can be visualised as a distinct, relatively sonolucent layer. In 30% to 50% of normal coron-

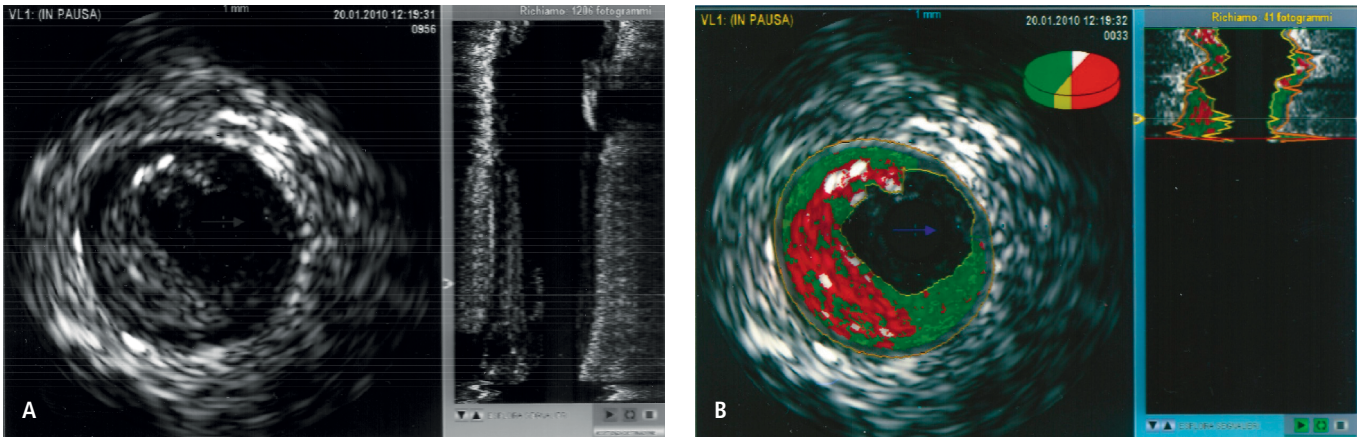

Figure 2: TFCA of the same plaque by IVUS and IVUS-VH. A) Gray-scale by IVUS. B) Image by IVUS-VH. Plaque composition: Red: necrotic core, Dark green: fibrous, Light green: fibro-fatty, White: calcified plaque.

ary arteries, the thin intima reflects ultrasound poorly, so it is not visualised as a separate layer (136-140). Lumen measurements are performed using the interface between the lumen and the leading edge of the intima (141).

Greyscale IVUS helps us to potentially determine vessel lumen size, distribution and severity of atherosclerotic plaque. In addition, it might be particularly useful in detecting the cross sectional area (142) (►Figure 2A). Lipid-laden lesions appear hypo echoic, fibro muscular lesions generate low-intensity or "soft" echoes, and fibrous or calcified lesions are relatively echogenic. Using IVUS Greyscale we can distinguish four kinds of plaques based on the acoustic signal (►Table 3) (143), considering that the echogenicity and texture of different tissue components may exhibit comparable acoustic properties and therefore appear quite similar. Thus, IVUS is helpful at determining the echogenicity of vessel wall structures but it is not consistently able to provide actual histology (140). In a recent study by Low et al., the accuracy of Greyscale IVUS in defining plaque characteristics *in vivo* has been analysed, using OCT. The sensitivity for IVUS detection of lipid content was 24.1%, and specificity 93.9%. Although detection of calcification had the highest reproducibility, its specificity was only intermediate (66.4%) with an excellent sensitivity (92.9%). The detection of a thin cap (defined as <65 μm) was difficult since the current best resolution of IVUS is 100 μm. The sensitivity and specificity of IVUS for detection of intraplaque calcifications were 92.9% vs 66.4%, respectively, while for disruption were 66.7% vs 96.1%. The authors concluded that Conventional Greyscale IVUS may not be a reliable imaging modality for detection of lipid-rich and hence vulnerable plaques (144). However, Yamagishi et al. demonstrated the increased risk of rupture of an eccentric atheroma with a relatively

Table 3: IVUS description of vulnerable plaque content.

Plaque morphology	Ultrasound appearance	Component of plaque	Limitations
1) Soft	Low echogenicity	High lipid content	It may also be: - a necrotic zone - an intramural hemorrhage
2) Fibrous	Intermediate echogenicity (the greater the fibrous tissue content, the greater the echogenicity of the tissue)	Fibrous tissue content	Very dense fibrous plaques may be misclassified as calcified
3) Calcium	Bright echoes that obstruct the penetration of sound (acoustic shadowing)	Calcium deposit content (described as superficial and deep)	- IVUS can detect only the leading edge and cannot determine the thickness of the calcium - reverberations or multiple reflections produced by Calcium
4) Mixed	More than one acoustic subtype	Mixed components content	Areas of heterogeneous signal cannot be reliably distinguished by Grey scale IVUS

Table 4: Colour code with VHIVUS and histological correlate.

Colour code	Red	White	Dark green	Yellow-green
Histological correlate	Necrotic core	Calcium	Fibrous	Fibro-fatty

large plaque burden, and a shallow echo lucent zone that was observed by Grey scale IVUS (145).

Although conventional Grey scale IVUS improved the field of percutaneous coronary intervention (PCI), its ability to distinguish plaque sub-types is limited by inter- and intra-observer subjectivity as well as by its axial resolution. Virtual histology intravascular ultrasound (VHIVUS) has moved the goal posts a little further by utilising similar principles to IVUS but allowing real-time quantification of plaque into differing subtypes. This technique uses similar equipment and ultrasound technology as the conventional Greyscale but employs spectral analysis to analyse the raw backscattered signal. VHIVUS uses autoregressive modelling to convert radiofrequency data into a power spectrum graph that plots the magnitude of the backscattered US signal against the frequency (142). Statistical classification trees sorted the radiofrequency data based on the combination of spectral parameters into one of four plaque components: fibrous, fibro-fatty, necrotic core and dense calcium (►Table 4 and ►Figure 2B). The initial model performed well with predictive accuracy of 90.4%, 92.8%, 90.9% and 89.5% for fibrous, fibro-fatty, calcified and calcified necrotic, respectively (146).

Pathological studies have shown that thrombotic coronary occlusion after the rupture of a lipid-rich atheroma with only a thin fibrous layer of intimal tissue covering the necrotic core (a thin-cap fibroatheroma) is the most common cause of myocardial infarction and death from cardiac causes (147-149). In this context, TCFA plaques with large avascular, hypocellular lipid cores seem particularly prone to rupture and result in epicardial occlusion (150-152). Using VHIVUS, Rodriguez-Granillo et al. (153) defined the IVUS-derived thin-cap fibroatheroma (IDTCFA) as a lesion that fulfills the following criteria in at least three consecutive frames: 1) necrotic core ≥10% without evident overlying fibrous tissue (the most accepted threshold to define a cap as "thin" has been set at 65 μm (154), but since the axial resolution of VHIVUS is between 100 and 150 μm, they assumed that the absence of visible fibrous tissue overlying a necrotic core suggested a cap thickness of below 100 to 150 μm and therefore used the absence of such tissue to define a thin fibrous cap (155), 2) percent atheroma volume ≥ 40%. In their *in vivo* study, Rodriguez-Granillo et al. found that IDTCFAs were more prevalent in patients with ACS compared to stable angina (153). Thus, IDTCFAs appear to be a reasonable surrogate of unstable plaques (154). In the PROSPECT Trial (36), that is one of the few longitudinal studies that test the evolution of vulnerable plaques into culprit lesions, among patients who presented with an ACS and underwent percutaneous coronary intervention, the investigators identified three characteristics of lesions that were significant predictors of subsequent events (►Table 5): 1) small luminal area (≤4.0 mm^2); 2) large plaque burden (≥70%); 3) the presence of a thin-cap fibroatheroma. In contrast, the absence of IDTCFA was also associated with relative stability, and lesions with a necrotic core of less than 10% had a negligible likelihood of causing major adverse cardiac event (MACE) at three years (154).

Table 5: Characteristics of "vulnerable plaque" in the PROSPECT trial [36]. *described by Rodriguez-Granillo et al. [152] as a lesion with: 1) necrotic core ≥10% without evident overlying fibrous tissue and 2) percent atheroma volume ≥ 40%.

1) Luminal area ≤4.0 mm^2
2) Plaque burden ≥70%
3) Presence of a thin-cap fibroatheroma*

Furthermore, IVUS was largely used to investigate the effect of anti-atherosclerotic drugs on coronary plaque geometry and/or plaque composition, mostly focused on statin therapy. A recent meta-analysis demonstrated that high doses and long duration of statin therapy is able to reduce the plaque volume and plaque composition in patients with stable angina and ACS (156). With regard to plaque composition, a regressive trend was seen for necrotic core volume but this did not induce a significant change in fibrotic, fibro-fatty, or dense calcium compositions.

Whereas IVUS was never found able to quantify the mechanical properties of vascular tissues, endovascular ultrasound elastography (IVUSe) was introduced to complement this technique. Nowadays IVUSe may be considered an emerging method that visualises the radial strain within vascular tissues. This technique assesses the local strain in the artery wall and in presence of plaques, using the phasic blood pressure change during the cardiac cycle as a natural force causing arterial tissue deformation. The principle is that in presence of soft material strain is higher than in presence of hard material. Thus, lipid-rich regions reveal significantly higher strain values than fibrous-rich regions. Therefore a thin fibrous cap atheroma is less able to sustain the circumferential stress applied on it with subsequent strain increase on the elastogram (157-160).

IVUS is also able to analyse additional intraplaque histological structures (such as the fibrous cap and the necrotic core) potentially associated with vulnerability. IVUS analysis of intraplaque histologic patterns has been described and listed in ►Table 3.

Calcium content

Although coronary calcification is a marker for future acute coronary events (160), the relationship between coronary calcification and plaque instability is controversial. In fact, although several IVUS studies have shown that unstable clinical symptoms are associated with less calcium (161, 162), Fujii et al. (163) suggested that even in patients who develop ACS as the first manifestation of CAD, coronary calcium is almost always present and usually exceeds the amount observed in asymptomatic patients or in those who have atypical symptoms. They demonstrated that ruptured

plaques had quantitatively less calcium, especially superficial calcium, but a larger number of small calcium deposits, especially deep calcium deposits. On the other hand, it has been reported that these calcified nodules may be considered as a histological feature of plaque vulnerability (25, 147, 164). Calcified nodules close to the luminal surface of the plaque can protrude through and break the fibrous cap, thus leading to thrombus formation and ACS. Calcified nodules are also seen in the post-mortem histopathological studies of patients who present with thrombosis and sudden coronary death (165). These studies demonstrated significantly different IVUS findings between calcified nodules and non-nodular calcium.

Vascular remodelling

Coronary arterial remodelling is the geometric alteration of the arterial wall in response to the progression or regression of atherosclerosis. Patterns of arterial remodelling have been shown to play an important role in both the progression of *de novo* atherosclerosis (166-168) and in the re-stenotic process following PCI (169, 170). Positive remodelling (PR) can be defined as an increase in vessel area, in contrast, negative or intermediate remodelling (NR/IR) can be defined as a decrease or no change in vessel area (171, 172).

Hong et al. defined a remodelling index >1.05 as a true PR, a remodelling index ≤1.05 and ≥0.95 as intermediate remodelling (IR), and a remodelling index <0.95 as negative remodelling (NR) (173). These authors demonstrated by VH-IVUS analysis that PR was associated with more vulnerable plaque components as compared IR/NR, regardless of their clinical presentation (►Table 4).

Plaque inflammation

Detection of macrophages within the fibrous cap requires a resolution within 10-20 μm. Considering that IVUS resolution is 10-20 times higher, it is impossible for IVUS to detect macrophages in atherosclerotic plaques (174).

Vasa vasorum (VV) neovascularisation

The VV are micro vessels that nourish the vessel walls (175, 176). Micro-computed tomography (MCT) and other methods have demonstrated that intraplaque VV appear in an early stage in the development of an atherosclerotic lesion and that this might contribute to plaque rupture at a later stage (177). Dynamic structural changes related to inflammation induce the VV network's enlarging in the adventitia and finally intraplaque neovascularisation, increasing the risk of IPH. IPH is believed to occur from the disruption of thin-walled microvessels that are lined by discontinuous endothelium without supporting smooth muscle cells (178). Microbubbles can be used to show the presence of VV in the atherosclerotic lesion. They can travel along the coronary arterial tree, reach its terminal network, and finally fill the VV (179). Then, microbubbles within the VV can then be detected by the returned echo-signals of the IVUS transducer (179-181).

Several studies have shown an enhanced adventitial signal in coronary arteries in porcine models for atherosclerosis using this system. Moreover, although the study by Vavuranakis et al. (178) showed the feasibility and safety of detecting microbubbles as they flow in the coronary lumen and as they reach the wall of non-culprit atherosclerotic plaques in patients with ACS, this technique is not yet ready for clinical use. For instance, high-quality software for three-dimensional reconstruction of VV remains to be developed (182). Once they have been developed, IVUS catheters and scanning methods will require regulatory approvals. Yet, developing a significant extension of the functionality of IVUS imaging is a promising prospect. In a near future, IVUS imaging of the coronary intraplaque VV might be used as an additional biomarker of plaque vulnerability.

Optical Coherence tomography (OCT) in plaque vulnerability

OCT is an intracoronary imaging modality similar to IVUS, but it uses near-infrared light instead of ultrasound (around 1,300 nm wavelength). Technically, it has a 10 times higher image resolution (10 to 20 μm) than conventional IVUS and has greater tissue contrast. Having better intraluminal image quality, OCT can distinguish three layers of the coronary artery wall, showing that the intima is the signal-rich layer nearest the lumen, the media is the signal-poor middle layer and the adventitia is the signal-rich layer surrounding the media (183). OCT is useful in evaluating plaque structure because it is able to microscopically analyse various components of the plaque, including fibrous cap thickness, macrophage infiltration and lipid content (184). It has also proven to be able to visualise microstructures near the lumen, such as calcified nodules, erosions and small thrombi (184-187). The following plaque characteristics can be assessed by OCT.

Fibrous cap thickness

Among all intravascular imaging diagnostics, OCT is the main modality with sufficient resolution to measure the thickness of the fibrous cap. Fibrous cap has been defined by OCT as the minimum axial distance from the coronary lumen to the inner border of the lipid pool, and its thickness can be measured at the thinnest portion in each plaque. Thin fibrous cap is one of the main characteristics of a TCFA (188, 189). In an observational study, Jang et al. (190) compared the OCT *in vivo* measures in a cohort of 57 patients symptomatic for recent AMI, ACS (including non-ST-segment elevation AMI [NSTEMI] and unstable angina), and stable angina pectoris (SAP), showing that TCFA was more frequent in patients with AMI or ACS. In an autopsy study, Kume et al. (191) confirmed that OCT imaging provided an accurate representation of the thickness of the fibrous cap with a Bland-Altman test that showed a mean difference of -24 ± 44 μm between the thicknesses of the fibrous cap measured on OCT and digitalised histological images. A study reported by Sawada et al. (192) that compared OCT to VH-IVUS demonstrated the superiority of OCT technology in this field. Despite this promising evidence, further studies

are needed before embracing thin cap OCT measurement as an elective imaging technique in the field of vulnerable rupture-prone plaques. Although 65 μm is the commonly used threshold to define thin fibrous cap, Yonetsu et al. claimed that this value may be inappropriate and requiring further investigations to confirm the correctness of this measure as a cut-off (193). These authors investigated the relationship between fibrous cap thickness and plaque rupture, studying 266 atherosclerotic lesions using OCT before PCI. They stated that in 95% of ruptured plaques, the thinnest cap thickness and most representative cap thickness were <80 and <188 μm, respectively, concluding that the widely accepted threshold of <65 μm for coronary plaque fibrous cap thickness may not be appropriate for identify *in vivo* rupture-prone plaques. Thus, prospective imaging studies are needed to better define this relevant aspect. Furthermore, the current methodology for determining fibrous cap thickness is derived from histology and is obtained by manual measurement at a single point or by averaging multiple measurements. Therefore, several new methods have recently been proposed to improve the accuracy of OCT in fibrous cap analysis. One of the most promising among them was reported by Wang et al. (194), who proposed a computer-aided method that is able to segment the boundaries and to show the three-dimensional (3D) morphology of the fibrous caps, thus providing complimentary information to the conventional metric. This method seems to be fast and could be used in future studies to achieve better characterisation of fibrous caps thereby improving our knowledge about the mechanisms leading to plaque rupture.

Macrophage infiltration

OCT allows for an improved definition of both the density and the distribution of inflammatory cells within the plaque. This is possible because intraplaque macrophages are relatively large cells (30-50 μm), might include lipids and contain a high degree of optical contrast. After measuring the intensity of the light reflected from the plaque by OCT, some authors described macrophages as a "bright spot" with high signal variance from the surrounding tissue of the plaque, and with different refracting indexes (195, 196). They reported a positive correlation between histological and OCT data, and showed that this technology is able to detect a cap CD68 density >10% with 100% sensitivity and specificity. These data show that OCT (together with ultra-small super paramagnetic iron oxides [USPIOs]) has a pivotal role in detecting inflammation within the plaque, which sets it apart from the other invasive technologies such as IVUS. Another notable advantage of OCT analysis of plaque inflammation is that it will likely improve our current knowledge about the physiopathology of plaque. In a recent three-vessel optical coherence tomography study, Kato et al. demonstrated that macrophage infiltration is not only a feature of the culprit lesion, but it is also observed in non-culprit lesions and non-culprit vessels, thus proving that inflammation in ACS plaques is a multifocal phenomenon (197). Despite these appealing capabilities, further studies are needed both to validate the criteria for identifying macrophages by OCT and to develop robust methods for macrophage quantification.

Lipid content

High lipid content plaques produce a low intensity signal with poorly defined border (198). However, despite the high resolution, one drawback of the current OCT systems is the limited penetration depth that does not allow the detection of lipid pools behind thick fibrous caps. Further, the main limitation of tissue characterisation by OCT is the inter- and intra-observer variation. Manfrini et al. analysed the inter-observer agreement the investigation of different plaque characteristics and concluded that the sensitivity of this technique in the detection of high lipid content plaque was 45% (199).

Plaque calcium content

Calcified lesions can be detected by OCT as a hypo signal region within the plaque (198). A problem that needs to be solved is that a signal-poor region within the plaque could be interpreted as a lipid area. It has been observed that the only difference is the image of the border: lipid content is often associated with diffuse borders, while calcium has sharp boundaries (198, 199). Thanks to this observation, OCT has high sensitivity (96%) and specificity (97%) in the detection of this type of lesion. An interesting advantage of OCT is its ability in 3D volumetric calcium characterisation which cannot be obtained by IVUS because of the limited penetration of ultrasound in calcium (200) and it is only indirectly detectable by Election Beam CT with low reproducibility (201). In fact, the authors showed that an analysis of the reproducibility had a mean variability of 19% for calcium score (calculated as the absolute rescan difference divided by the mean calcium score, multiplied by 100) (201).

It is also possible to detect superficial micro-calcifications, a distinctive feature of plaque vulnerability, as small superficial calcium deposits. Furthermore, it is also interesting when having to choose a revascularisation technique since lesions with high calcium content are associated with higher rates of stent malposition (202).

Plaque rupture/erosions

The "rupture" of an atherosclerotic plaque implies the discontinuity in the fibrous cap that connects lumen with the lipid pool causing the formation of a cavity within the plaque, while the "erosion" has been defined as the loss of endothelial continuity with no cavity formation (203). The reported ability of OCT to detect plaque erosions varies in different studies. Jang et al. reported that rupture was detectable by OCT in only 25% of their patients with STEMI (190). In a recent study, Stefano et al. analysed the role of FD-OCT, a promising new OCT technology in the evaluation of intermediate coronary artery stenosis, and observed that none of the ACS patients had plaque rupture or erosion depicted by FD-OCT in the suspected "culprit" vessels (204). On the other hand, Kubo et al. observed that rupture/erosion was detectable by OCT in 73% of their AMI patients (205). In 2009, a study showed that the rate of fibrous cap erosion detected by OCT in a group of unstable angina

patients was significantly higher than in the SAP group (59% vs 9%) (206). The frequency of plaque rupture and erosion detected by OCT differs significantly, even among different types of unstable angina patients as shown by Mizukoshi et al. (207). A possible explanation for the different results of these studies might be the differences in the amount of time that elapsed between clinical presentation and image capture. Further investigations are needed to determine the ability of OCT in detecting plaque rupture/erosion, as well as the ideal interval of time between clinical presentation and image capture, and its potential clinical implications.

Coronary thrombi

The high resolution of OCT even allows a thrombus to be detected and characterised as red or white. Jang et al. showed that the detection rate of thrombotic material using IVUS is significantly lower than using OCT in patients presenting with AMI (208). Thrombus is identified as masses protruding into the vessel lumen from the surface of the wall. Red thrombi consist mainly of red blood cells and fiber content and the light cannot penetrate them. Thus, relevant OCT images are characterised as high-backscattering protrusions with signal-free shadowing, while white thrombi, consisting of platelets, are characterised by signal-rich, low-backscattering billowing projections protruding into the lumen (143, 209). Recently, Bezerra et al. observed that OCT lacks the ability to distinguish a thrombus from other abnormal intraluminal phenomena. Additionally, despite the high resolution of OCT, the presence of residual blood in the vessel during a procedure can lead to an artifact that might be erroneously identified as a thrombus (210).

Arterial remodelling

There is limited literature studying OCT plaque characterisation and remodelling. Considering its limited tissue penetration (1-1.5 mm), OCT does not appear to be useful to study vessel remodelling in the presence of a large plaque burden. In fact, OCT does not penetrate sufficiently to allow visualisation of the media (183). However, Kume et al. evaluated the relationship between coronary arterial remodelling as assessed by IVUS and plaque morphology studied by histological examination (211). They also compared the morphology between histopathology and OCT imaging, showing higher lipid content and larger plaque area in lesions with positive remodelling along with other characteristics of vulnerable plaque and ruptured plaques. Few other studies (212, 213) have analysed the role of OCT in the detection of arterial remodelling, showing a correlation with several characteristics of vulnerable plaque. Further investigations are needed to validate the criteria for identifying this aspect by OCT and to develop a standardised method for remodelling quantification.

Limitations to the clinical application of invasive imaging techniques

A great challenge in the next few years will be to improve the ability of OCT to distinguish certain plaque characteristics, such as the differentiation between lipid and calcium content or precise identification of thrombotic material. This light-based energy technology also has poor tissue penetration depth (2 to 3 mm), thus giving OCT a lower capability to measure the size of the vessel and the area of the plaque under study as compared to IVUS (207). Furthermore, during the procedure a blood free imaging zone is needed. This is achievable through intermittent saline flushes from the guiding catheter. With this flushing technique and the image acquisition speed of current OCT systems, it is not possible to detect long arterial segments, and image acquisition is still complex. Despite these limitations, the high resolution of OCT provides more detailed structural information of the coronary artery compared with conventional imaging modalities, particularly in the detection of TCFA with inflammation, making OCT a great device in the field of vulnerable plaques and giving this imaging technique a bright future (206, 214). A second OCT generation (named frequency-domain OCT [FD-OCT]) might improve the precise identification of a rupture-prone atherosclerotic plaque. Thanks to a greater number of lines per frame (OCT vs FD-OCT:

Table 6: Comparison between invasive and noninvasive imaging methods to study a vulnerable plaque.

	CT	MRI	FDG-PET	VH-IVUS	OCT
Spatial resolution	+++	+++	+	++	++++
Specificity	+	++	++	++	++
Sensitivity	+	++	++	++	+++
Plaque morphology	+++	++	-	+++	++
Penetration	++++	++++	+	+++	+
Coronary imaging	+	±	-	+	-
Clinical use	+++	++	-	+++	+
Radiation	++	-	+++	-	-
Side effects and specific features	Nephrotoxicity due to the contrast agent, radiation exposure	Systemic fibrosis due to the contrast agent	Radiation exposure	Invasive	Invasive

200 vs 450), higher frame rate imaging (OCT vs FD-OCT: 15.6 vs 100 f/sec), pullback/speed (OCT vs FD-OCT: 1.0-2-0 vs 20 mm/sec) and a simpler acquisition of spectroscopic and polarisation data (215-218), this new technology allows a more precise characterisation of the vessel's wall. In combination with a short, non-occlusive flush of rapid spiral pullback, the higher frame rates enable to show the 3D microstructure of the plaque (219). However, the clinical use of FD-OCT to evaluate plaque features and severity of lumen stenosis require additional investigations.

Conclusions and future perspectives

Several studies have been carried out on vulnerable plaque as the main culprit of major adverse cardiac events. Therefore, in our opinion defining the most appropriate invasive and non-invasive imaging techniques to identify "high-risk plaque" remains a great challenge. In this review, we focused on the main characteristics of invasive and non-invasive methods (►Table 6).

As discussed above, CT may be considered the most accurate clinical method for non-invasive coronary stenosis detection (40, 220). However, a suboptimal tissue contrast and the radiation exposure rendered CT a less suitable candidate for vulnerable plaque imaging (220). Nuclear techniques stand out because of their high sensitivity which allows us to detect sparse targets in the nanomolar range using a low tracer dose, but these modalities have limited spatial resolution (PET: 1-2 mm, SPECT: 0.3-1 mm), considering the small size of the region of interest for target localisation in a beating heart. Although not currently available for routine use *in vivo*, multi-contrast MRI remains the most promising non-invasive method for the imaging of vulnerable plaque in carotid arteries, thanks to the absence of ionising radiation and the high spatial resolution, even if its application is limited to large arteries. Imaging of the coronary arteries remains challenging due to the limited temporal resolution that hampers its application in the coronary circulation. However, new contrast agents targeting plaque components (such as endothelial cells or inflammatory cells) as well as molecular approaches are becoming available for MRI and other imaging modalities, and these data will improve clinical applications in the diagnosis, prevention and treatment of atherosclerosis.

IVUS and OCT are two different techniques that are used to evaluate coronary plaques. Unfortunately, both methods have various limits in the correct detection of thin-cap fibroatheroma. Thus, it is difficult to diagnose TCFA using each of the modalities alone. Although a combination of complementary tools such as VH-IVUS and OCT might be a feasible approach for more accurate detection of TCFA, the combined use of the two techniques appears laborious and costly. However, the combined use of VH-IVUS and OCT could be a key tool for characterising the coronary model of future events (221). Moreover, a new device with both IVUS and OCT functions should be developed to enable the simultaneous use of both modalities.

To date, no single technique is able to precisely predict atheroprogression and the final clinical rupture. In contrast, the integration of data that can be derived from multiple methods might improve our knowledge about plaque destabilisation. However, at present, this promising clinical approach is limited due to cost and logistic reasons. Future studies have to focus not only on the possible development of each single technique, but they will also have to look into the integration of the techniques in order to optimise the approach in clinical practice.

Conflicts of interest
None declared.

References

1. Brevoord D, et al. Remote ischaemic conditioning to protect against ischaemia-reperfusion injury: a systematic review and meta-analysis. PLoS One 2012; 7: e42179.
2. Libby P, Theroux P. Pathophysiology of coronary artery disease. Circulation 2005; 111: 3481-3488.
3. Falk E, et al. Coronary plaque disruption. Circulation 1995; 92: 657-671.
4. Moreno PR, et al. Promoting mechanisms of vascular health: circulating progenitor cells, angiogenesis, and reverse cholesterol transport. J Ann Coll Cardiol 2009; 53: 2315-2323.
5. Schaar JA, et al. Terminology for high risk and vulnerable coronary artery plaques. Report of a meeting on the vulnerable plaque. June 17 and 18, 2003, Santorini, Greece. Eur Heart J 2004; 25: 1077-1082.
6. Loree HM, et al. Effects of fibrous cap thickness on peak circumferential stress in model atherosclerotic vessels. Circ Res 1992; 71: 850-858.
7. Richardson PD, et al. Influence of plaque configuration and stress distribution on fissuring of coronary atherosclerotic plaques. Lancet 1989; 2: 941-944.
8. Cheng GC, et al. Distribution of circumferential stress in ruptured and stable atherosclerotic lesions: a structural analysis with histopathological correlation. Circulation 1993; 87: 1179-1187.
9. Naghavi M, et al. From vulnerable plaque to vulnerable patient: a call for new definitions and risk assessment strategies: Part II. Circulation 2003; 108: 1772-1778.
10. Zethelius B, et al. Use of multiple biomarkers to improve the prediction of death from cardiovascular causes. N Eng J Med 2008; 358: 2107-2116.
11. Shaub N, et al. Markers of plaque instability in the early diagnosis and risk stratification of acute myocardial infarction. Clin Chem 2012; 58: 246-256.
12. Ferroni P, et al. Biomarkers of platelet activation in acute coronary syndromes. Thromb Haemost 2012; 108: 1109-1123.
13. Flierl U, Schafer A. Fractalkine - a local inflammatory marker aggravating platelet activation at the vulnerable plaque. Thromb Haemost 2012; 108: 457-463.
14. Alsheikh-Ali AA, et al. The vulnerable atherosclerotic plaque: scope of the literature. Ann Intern Med 2010; 153: 387-395.
15. Naghavi M, et al. From vulnerable plaque to vulnerable patient: a call for new definitions and risk assessment strategies: Part I. Circulation 2003; 108: 1664-1672.
16. Muller JE, et al. Circadian variation in the frequency of onset of acute myocardial infarction. N Eng J Med 1985; 313: 1315-1322.
17. Kolodgie FD, et al. Pathologic assessment of the vulnerable human coronary plaque. Heart 2004; 90: 1385-1391.
18. Virmani R, et al. Pathology of the vulnerable plaque. J Am Coll Cardiol 2006; 47: C13-C18.
19. Narula J, et al. Arithmetic of vulnerable plaques for noninvasive imaging. Nat Clin Pract Cardiovasc Med 2008; 5: s2-10.
20. Falk E. Pathogenesis of atherosclerosis. J Am Coll Cardiol 2006; 47: C7-12.
21. Yla-Herttuala, et al. Stabilisation of atherosclerotic plaques. Thromb Haemost 2011; 106: 1-19.
22. Loree HM, et al. Effects of fibrous cap thickness on peak circumferential stress in model atherosclerotic vessels. Circ Res 1992; 71: 850-858.
23. Schaar JA, et al. Intravascular palpography for vulnerable plaque assessment. J Am Coll Cardiol 2006; 47: C86-91.
24. Moreno PR. Vulnerable plaque: definition, diagnosis and teatment. Clin Cardiol 2010; 28: 1-30.

25. Davies MJ. The pathophysiology of acute coronary syndromes. Heart 2000; 83: 361-366.
26. Felton CV, et al. Relation of plaque lipid composition and morphology to the stability of human aortic plaques. Aterioscler Thromb Vasc Biol 1997; 17: 1337-1345.
27. Fuster V, et al. Atherothrombosis and high-risk plaque part I: evolving concepts. J Am Coll Cardiol 2005; 46: 937-954.
28. Waxman S, et al. Detection and treatment of vulnerable plaques and vulnerable patients: novel approaches to prevention of coronary events. Circulation 2006; 114: 2390-2411.
29. Kockx MM, et al. Phagocytosis and macrophage activationassociated with hemorrhagic microvessels in human atherosclerosis. Atherioscler Thromb Vasc Biol 2003; 23: 440-446.
30. Kolodgie FD, et al. Intraplaque Hemorrhage and progression of coronary atheroma. N Eng J Med 2003; 349: 2316-2325.
31. Michel JB, et al. Intraplaque Hemorrhages as the trigger of plaque vulnerability. Eur Heart J 2011; 32: 1977-1985.
32. Arbustini E, et al. Plaque composition in plexogenic and thromboembolic pulmonary hypertension: the critical role of thrombotic material in pultaceous core formation. Heart 2002; 88: 177-182.
33. Moreno PR, et al. Intimomedial interface damage and adventitial inflammation interface damage and adventitial inflammation is increased beneath disrupted atherosclerosis in the aorta: implications for plaque vulnerability. Circulation 2002; 105: 2504-2511.
34. Tronc F, et al. Role of matrix metalloproteinases in blood flow-induced arterial enlargement: interaction with NO. Arterioscler Thromb Vasc Biol 2000; 20: E120-126.
35. Bruke AP, et al. Morphological predictors of arterial remodelling in coronary atherosclerosis. Circulation 2002; 105: 297-303.
36. Stone GW, et al., for the PROSPECT Investigators. A prospective natural-history study of coronary atherosclerosis. N Engl J Med 2011; 364: 226-235.
37. Corti R, et al. New understanding of atherosclerosis (Clinically and experimentally) with evolving MRI technologies in vivo. Ann NY Acad Sci 2001; 947: 181-195.
38. Achenbach S, et al. Detection of coronary artery stenoses by contrast-enhanced, retrospectively electrocardiographically gated, multislice spiral computed tomography. Circulation 2001; 103: 2535-2538.
39. Leschka S, et al. Optimal image reconstruction intervals for non–invasive coronary angiography wit 64-slice CT. Eur Radiol 2006; 16: 1964-1972.
40. Vanhoenacker PK, et al. Diagnostic performance of multidetector CT angiography for assessment of coronary artery disease: meta-analysis. Radiology 2007; 244: 419-428.
41. Kido T, et al. Cardiac imaging using 256-detector row four dimensional CT: preliminary clinical report. Radiat Med 2007; 25: 38-44.
42. Hendel RC, et al. ACCF/ACR/SCCT, SCMR, ASNC, NASCI, SCAI, SIR 2006 appropriateness criteria for cardiac computed tomography and cardiac magnetic resonance imagin: a report of the American College of Cardiology Foundation Quality Strategy Directions Committee Appropriateness Criteria Working Group, American College of Radiology , Society of Cardiovascular Computed Tomography, Society of Cardiovascular Magnetic Resonance, American Society of Nuclear Cardiology, North American Society for Cardiac Imaging, Society for Cardiovascular Angiography and Interventions and Society of Interventional Radiology. J Am Coll Cardiol 2006; 48: 1475-1497.
43. Schroeder S, et al. Cardiac computed tomography: indications, applications, limitations and training requirements. Eur Heart J 2008; 29: 531-536.
44. Inoue K, et al. Serial Coronary CT Angiography–Verified Changes in Plaque Characteristics as an End Point. Evaluation of Effect of Statin Intervention. JACC Cardiovasc Imaging 2010; 3: 691-698.
45. Ehara S, et al. Spotty calcification typifies the culprit plaque in patients with acute myocardial infarction: an intravascular ultrasound study. Circulation 2004; 110: 3424-3429.
46. Pundziute G, et al. Head-to-head comparison of coronary plaque evaluation between multislice and intravascular ultrasound radiofrequency data analisis. JACC Cardiovasc Imaging 2008: 1: 176-182.
47. Camici PG, et al. Non-invasive anatomic and functional imaging of vascular inflammation and unstable plaque. Eur Heart J 2012; 33: 1309-1317.
48. Leber AW, et al. Composition of coronary atherosclerotic plaques in patients with acute myocardial infarction and stable angina pectoris determined by contrast enhanced multislice computed tomography. Am J Cardiol 2003; 91: 714-718.
49. Hoffmann U, et al. Noninvasive assessment of plaque morphology and composition in culprit and stable lesions in acute coronary syndrome and stable lesions in stable angina by multidetector computed tomography. J Am Coll Cardiol 2006; 47: 1655-1662.
50. Motoyama S, et al. Multislice computed tomographic characteristics of coronary lesions in acute coronary syndromes. J Am Coll Cardiol 2007; 50: 319-326.
51. Motoyama S, et al. Computed tomography characteristics of atherosclerotic plaques subsequently resulting in acute coronary syndromes. J Am Coll Cardiol 2009; 54: 49-57.
52. Kashiwagi M, et al. Feasibility on noninvasive assessment of thin-cap fibroatheroma by multidetector computed tomography. JACC Cardiovasc Imaging 2009; 2: 1412-1419.
53. Maurovich-Horvat P, et al. The napkin-ring sign: CT signature of high-risk coronary plaques? JACC Cardiovasc Imaging 2010; 3: 440-444.
54. Pflederer T, et al. Characterisation of culprit lesions in acute coronary syndromes using coronary dual-source CT angiography. Atherosclerosis 2010; 211: 437-444.
55. Hyafil F, et al. Noninvasive detection of macrophages using a nanoparticulate contrast agent for computed tomography. Nat Med 2007; 13: 636-641.
56. Hyafil F, et al. Quantification of inflammation with rabbit atherosclerotic plaques using the macrophage–specific CT Contrast agent N1177: a comparison wit 18FDG PET/CT and histology. J Nucl Med 2009; 50: 959-965.
57. Weissleder R, Mahmood U. Molecular imaging. Radiology 2001; 219: 316-333.
58. Cormode DP, et al. Atherosclerotic plaque composition analysis with multicolour CT and targeted gold nanoparticles. Radiology 2010; 256: 774-782.
59. Choudhury RP, et al. Molecular, cellular and functional imaging of atherothrombosis. Nat Rev Drug Discv 2004; 3: 913-925.
60. Yuan C, et al. Carotid atherosclerotic plaque: non invasive MR characterisation and identification of vulnerable lesions. Radiology 2001; 221: 285-299.
61. Yuan C, et al. In vivo accuracy of multispectral magnetic resonance imaging for identifying lipid rich necrotic cores and intraplaque hemorrhage in advanced human carotid plaques. Circulation 2001; 104: 2051-2056.
62. Saam T, et al. The vulnerable or high-risk, atherosclerotic plaque: non-invasive MR imaging for characterisation and assessment. Radiology 2007; 244: 64-77.
63. Demarco JK, et al. MR carotid plaque imaging and contrast-enhanced MR angiography identifies lesions associated with recent ipsilateral throembolic symptoms: an in vivo study at 3T. Am J Neuroradiol 2010; 31: 1395-1402.
64. Takaya N, et al. Association between carotid plaque characteristics and subsequent ischaemic cerebrovascular: a prospective assessment with MRI-initial results. Stroke 2006; 37: 818-823.
65. Sadat U, et al. High resolution magnetic resonance imaging-based biochemical stress analysis of carotid atheroma: a comparison of single transient ischaemic attack, recurrent transient ischaemic attacks, non-disabling stroke and asymptomatic patients group . Eur J Vasc Endovasc Surg 2011; 41: 83-90.
66. Murphy RE, et al. Characterisation of complicated carotid plaque with magnetic resonance direct thrombus imaging in patients with cerebral ischaemia. Circulation 2003; 107: 3047-3052.
67. Zhao X, et al. Discriminating carotid atherosclerotic lesion severity by luminal stenosis and plaque burden. Stroke 2011; 42: 347-353.
68. Saam T, et al. Comparison of symptomatic and asymptomatic atherosclerotic carotid plaque features with in vivo MR imaging. Radiology 2006; 240: 464-472.
69. Singh N, et al. Moderate carotid artery stenosis: MR imaging-depicted intraplaque hemorrhage predicts risk of cerebrovascular ischaemic events in asymptomatic men. Radiology 2009; 252: 502-508.
70. Kolodgie FD, et al. Elimination of neoangiogenesis for plaque stabilisation: is there a role for local drug therapy? J Am Coll Cardiol 2007; 49: 2093-2101.
71. Cappendijk VC, et al. In vivo detection of hemorrhage in human atherosclerotic plaques with magnetic resonance imaging. J Magn Reson I 2004; 20: 105-110.
72. Cappendijk VC, et al. Assessment of human atherosclerotic carotid plaque components with mulsequence MR imaging initial experience. Radiology 2005; 234: 487-492.
73. Sullivan JL. Iron and sex difference in heart disease risk. Lancet 1981; 1: 1293-1294.
74. Raman SV, et al. In vivo atherosclerotic plaque characterisation using magnetic susceptibility distinguished symptom producing plaques. JACC Cardiovasc Imaging 2008; 1: 49-57.

75. Camici PG, et al. Non invasive anatomic and functional imaging of vascular inflammation and unstable plaque. Eur Heart J 2012; 33: 1309-1317
76. Wasserman BA, et al. Carotid artery atherosclerosis in vivo morphologic characterisation with gadolinium/enhanced double oblique MR imaging /initial results. Radiology 2002; 223: 566-573.
77. Yuan C, et al. Contrast enhanced high resolution MRI for atherosclerotic carotid artery tissue characterisation. J Magn Reson Imaging 2002; 15: 62-67.
78. Choudhury RP, et al. Molecular, cellular and functional imaging of atherotrombosis. Nat Rev Drug Discover 2004; 3: 913-925.
79. Kerwin WS, et al. Inflammation in carotid atherosclerotic plaque : a dynamic contrast –enhanced MR imaging study. Radiology 2006; 241: 459-468.
80. Trivedi RA, et al. Identifying inflamed carotid plaques using in vivo USPIO-enhanced MR imaging to label plaque macrophages . Arterioscler Thromb Vasc Biol 2006; 26: 1601-1606.
81. Chu B, et al. Magnetic resonance imaging features of the disruption-prone and the disrupted carotid plaque. JACC Cardiovasc Imaging 2009; 2: 883-896.
82. Corti R, et al. Effects of lipid-lowering by simvastatin on human atherosclerotic lesions: a longitudinal study by high resolution, non invasive magnetic resonance imaging. Circulation 2001; 104: 249-252.
83. Corti R, et al. Effects of aggressive versus conventional lipid-lowering therapy by simvastatin on human atherosclerotic lesions: a prospective randomized, double-blind trial with high-resolution magnetic resonance imaging. J Am Coll Cardiol 2005; 46: 106-112.
84. Zhao XQ, et al. Effects of prolonged intensive lipid-lowering therapy on the characteristics of carotid atherosclerotic plaques in vivo by MRI: a case control study. Arterioscler Thromb Vasc Biol 2001; 21: 1623-1629.
85. Underhill HR, et al. Effect of rosuvastatin therapy on carotid plaque morphology and composition in moderately hypercoesterolemic patients. A high-resolution magnetic resonance imaging trial . Am Heart J 2008; 155: 584e1-e8.
86. Tang TY, et al. Temporal dependence of in vivo USPIO-enhancement MRI signal changes in human atheromatous carotid plaques. Neuroradiol 2009; 51: 457-465.
87. Yun M, et al. F-18FDG uptake in the large arteries: a new observation. Clin Nucl Med 2001; 26: 314-319.
88. Rudd JH, et al. Imaging atherosclerotic plaque inflammation with [18F]-fluorodeoxyglucose positron emission tomography. Circulation 2002; 105: 2708-2711.
89. Tawakol A, et al. In vivo 18F-fluorodeoxyglucose positron emission tomography imaging provides a noninvasive measure of carotid plaque inflammation in patients. J Nucl Cardiol 2005; 12: 294-301.
90. Rudd JH, et al. (18)Fluorodeoxyglucose positron emission tomography imaging of atherosclerotic plaque inflammation is highly reproducible: implications for atherosclerosis therapy trials. J Am Coll Cardiol 2007; 50: 892-896.
91. Mauriello A, et al. Diffuse and active inflammation occurs in both vulnerable and stable plaques of the entire coronary tree: a hystophatologic study of patients dying of acute myocardial infarction. J Am Coll Cardiol 2005; 45: 1585-1593.
92. Tahara N, et al. Simvastatin attenuates plaque inflammation. Evaluation by fluorodeoxyglucose positron emission tomography. J Am Coll Cardiol 2006; 48: 1825-1831.
93. Wykrzykowska J, et al. Imaging of inflamed and vulnerable plaque in coronary arteries with 18-FDG PET/CT in patients with suppression of myocardial uptake using a low-carbohydrate, high-fat preparation. J Nucl Med 2009; 50: 563-568.
94. Rogers IS, et al. Feasibility of FDG imaging of the coronary arteries: comparison between acute coronary syndrome and stable angina. J Am Coll Cardiol Img 2010; 3: 388-397.
95. Rominger A, et al. 18FDG-PET/CT identifies patients at risk for future vascular events in an otherwise asymptomatic cohort with neoplastic disease. J Nucl Med 2009; 50: 1611-1620.
96. Camici PG, et al. Non-invasive anatomic and functional imaging of vascular inflammation and unstable plaque. Eur Heart J 2012; 33: 1309-1317.
97. Matter CM, et al. 18F-choline images murine atherosclerotic plaques ex viv. Artherioscler Thromb Vasc Biol 2006; 260: 584-589.
98. Bucerius J, et al. Feasibility of 18F-fluoromethylcholine PET/CT for imaging of vessel wall alterations in humans—first results. Eur J Nucl Med Mol Imaging 2008; 35: 815-820.
99. Dweck MR, et al. Coronary arterial 18F-Sodium Fluoride Uptake. A novel marker of plaque biology. J Ann Coll Cardiol 2012; 59: 1539-1548.
100. Soloperto G, Casciaro S. Progress in atherosclerotic plaque imaging. World J Radiol 2012; 4: 353-371.
101. Johnson LL, et al. 99mTc-annexin V imaging for in vivo detection of atherosclerotic lesions in porcine coronary arteries. J Nucl Med 2005; 46: 1186-1193.
102. Isobe S, et al. Noninvasive imaging in atherosclerotic lesions in apolipoprotein E-deficient and low-density-lipoprotein receptor-deficient mice with annexin A5. J Nucl Med 2006; 47: 1497-1505.
103. Ishino S, et al. 99mTc-Annexin A5 for noninvasive characterisation of atherosclerotic lesions: imaging and histological studies in myocardial infarction-prone Watanabe heritable hyperlipidemic rabbits. Eur J Nucl Med Mol Imaging 2007; 34: 889-899.
104. Kietselaer BL, et al. The role of labeled Annexin A5 in imaging of programmed cell death. From animal to clinical imaging. Q J Nucl Med 2003; 47: 349-361.
105. Hartung D, et al. Resolution of apoptosis in atherosclerotic plaque by dietary modification and statin therapy. J Nucl Med 2005; 46: 2051-2056.
106. Elkhaward M, Rudd JHF. Radiotracer imaging of atherosclerotic plaque biology. Cardiol Clin 2009; 27: 345-354.
107. Sakalihasan N, Michel JB. Functional Imaging of Atherosclerosis to Advance Vascular Biology. Eur J Vasc Endovasc Surg 2009; 37: 728-734.
108. Ogawa M, et al. Application of 18F-FDG PET for monitoring the therapeutic effect of antiinflammatory drugs on stabilisation of vulnerable atherosclerotic plaques. J Nucl Med 2006; 47: 1845-1850.
109. Iuliano L, et al. Preparation and biodistribution of 99m-technetium labelled oxidized LDL in man. Atherosclerosis 1996; 126: 131-141.
110. Ishino S, et al. Targeting of Lectinlike Oxidized Low-Density Lipoprotein Receptor 1 (LOX-1) with 99mTc-Labeled Anti–LOX-1 Antibody: Potential Agent for Imaging of Vulnerable Plaque. J Nucl Med 2008; 49: 1677-1685.
111. Li D, et al. Molecular Imaging of Atherosclerotic Plaques Targeted to Oxidized LDL Receptor LOX-1 by SPECT/CT and Magnetic Resonance. Circ Cardiovasc Imaging 2010; 3: 464-472.
112. Hardoff R, et al. External imaging of atherosclerosis in rabbits using an 123I-labeled syntetic peptide fragment. J Clin Pharmacol 1993; 33: 1039-1047.
113. Demacker PN, et al. Evaluation of indium-111-polyclonal immunoglobulin G to quantitate atherosclerosis in Watanabe heritable hyperlipidemic rabbits with scintigraphy: effect of age and treatment with antioxidants or ethinylestradiol. J Nucl Med 1993; 34: 1316-1321.
114. Chakrabarti M, et al. Biodistribution and radioimmunopharmacokinetiks of 131I-Ama monoclonal antibody in atherosclerotic rabbits. Nucl Med Biol 1995; 22: 693-697.
115. Narula J, et al. Noninvasive localisation of experimental atherosclerotic lesions with mouse/human chimeric Z2D3 F(ab')2 specific for the proliferating smooth muscle cells of human atheroma. Imaging with conventional and negative charge-modified antibody fragments. Circulation 1995; 92: 474-484.
116. Carrio I, et al. Noninvasive localisation of human atherosclerotic lesions with indium 111-labeled monoclonal Z2D3 antibody specific for proliferating smooth muscle cells. J Nucl Cardiol 1998; 5: 551-557.
117. Ohtsuki K, et al. Detection of monocyte chemoattractant protein-1 receptor expression in experimental atherosclerotic lesions: an autoradiographic study. Circulation 2001; 104: 203-208.
118. Bidzhekov K, et al. MCP-1 induces a novel transcription factor with proapoptotic activity. Circ Res 2006; 98: 1107-1109.
119. Shah PK, et al. Human Monocyte-Derived Macrophages Induce Collagen Breakdown in Fibrous Caps of Atherosclerotic Plaques: Potential Role of Matrix- Degrading Metalloproteinases and Implications for Plaque Rupture. Circulation 1995; 92: 1565-1569.
120. Chenga C, et al. Activation of MMP8 and MMP13 by angiotensin II correlates to severe intra-plaque hemorrhages and collagen breakdown in atherosclerotic lesions with a vulnerable phenotype. Atherosclerosis 2009; 204: 26-33.
121. Xie S, et al. Inhibiting extracellular matrix metalloproteinase inducer maybe beneficial for diminishing the atherosclerotic plaque instability. J Postgrad Med 2009; 55: 284-286.
122. Fujimoto S, et al. Molecular imaging of matrix metallo- proteinase in atherosclerotic lesions: resolution with dietary modification and statin therapy. J Am Coll Cardiol 2008; 52: 1847-1857.
123. Haider N, et al. Dual molecular imaging for targeting metalloproteinase activity and apoptosis in atherosclerosis: molecular imaging facilitates understanding of pathogenesis. J Nucl Cardiol 2009; 16: 753-762.

124. Ohshima S, et al. Molecular imaging of matrix metallopro- teinase expression in atherosclerotic plaques of mice deficient in apolipoprotein e or low-density-lipoprotein receptor. J Nucl Med 2009; 50: 612–617.
125. Kuge Y, et al. Imaging with radiolabelled anti-membrane type 1 matrix metalloproteinase (MT1-MMP) antibody: potentials for characterising atherosclerotic plaques. Eur J Nucl Med Mol Imaging 2010; 37: 2093-2104.
126. Razavian M, et al. Atherosclerosis Plaque Heterogeneity and Response to Therapy Detected by In Vivo Molecular Imaging of Matrix Metallo- proteinase Activation. J Nucl Med 2011; 52: 1795-1802.
127. Lenglet S, et al. Molecular imaging of matrix metalloproteinases in atherosclerotic plaques. Thromb Haemost 2012; 107: 409-416.
128. Wagner S, et al. The MMP inhibitor (R)-2-(N-benzyl-4-(2-[18F]fluoroethoxy)phenylsulphonamido)-N-hydroxy-3-methylbutanamide: Improved precursor synthesis and fully automated radiosynthesis. Appl Radiat Isot 2011; 69: 862-868.
129. Beller GA. Imaging of vulnerable plaques: will it affect patient management and influence outcomes? J Nucl Cardiol 2011; 18: 531-533.
130. Bom N, Lancee CT. 1972 Apparatus for ultrasonically examining a hollow organ. UK Patent no. 1402192.
131. Bom N, et al. The technical potential of IVUS: history and principles. In: Vascular ultrasound, Springer 2003; Tokyo, Japan; pp. 51-65.
132. de Korte CL, et al. Vascular ultrasound for atherosclerosis imaging. Interface Focus 2011; 1: 565-575.
133. Nissen SE, Yock P. Intravascular ultrasound: novel pathophysiological insights and current clinical applications. Circulation 2001; 103: 604-616.
134. Rodriguez-Granillo GA, et al. In vivo variability in quantitative coronary ultrasound and tissue characterisation measurements with mechanical and phased-array catheters. Int J Cardiovasc Imaging 2006; 22: 47-53.
135. Goar FG, et al. Intravascular ultrasound imaging of angiographically normal coronary arteries: an in vivo comparison with quantitative angiography. J Am Coll Cardiol 1991; 18: 952-958.
136. Gussenhoven EJ, et al. Arterial wall characteristics determined by intravascualar ultrasound imaging: an in vitro study. J Am Coll Cardiol 1989; 14: 947-952.
137. Potkin BN, et al. Coronary artery imaging with intravascular high-frequency ultrasound. Circulation 1990; 81: 1575-1585.
138. Nishimura RA, et al. Intravascular ultrasound imaging: in vitro validation and patologic correlation. J Am Coll Cardiol 1990; 16: 145-154.
139. Nissen SE, Yock P. Intravascular Ultrasound: Novel Pathophysiological Insights and Current Clinical Applications. Circulation 2001; 103: 604-616.
140. Mintz GS, et al. American College of Cardiology clinical expert consensus document on standards for acquisition measurements and reporting of intravascular ultrasound studies (IVUS). A report of the American College of Cardiology Task Force on Clinical Expert Consensus Documents. J Am Coll Cardiol 2001; 37: 1478-1492.
141. Layland J, et al. Virtual Histology: A Window to the Heart of Atherosclerosis. Heart Lung Circ 2011; 20: 615-621.
142. Kume T, et al. Assessment of coronary arterial thrombus by optical coherence tomography. Am J Cardiol 2006; 97: 1713-1717.
143. Low AF, et al. In vivo characterisation of coronary plaques with conventional grey-scale intravascular ultrasound: correlation with optical coherence tomography. EuroIntervention 2009; 4: 626-632.
144. Yamagishi M, et al. Morphology of Vulnerable Coronary Plaque: Insights from Follow-up of patients Examined by Intravascula Ultrasound Before an Acute Coronary Syndrome. J Am Coll Cardiol Vol 2000; 35: 106-111.
145. Nair A, et al. Coronary plaque classification with intravascular ultrasound radiofrequency data analysis. Circulation 2002; 106: 2200-2206.
146. Virmani R, et al. Pathology of the vulnerable plaque. J Am Coll Cardiol 2006; 47: C13-C18.
147. Ishikawa Y, et al. Histopathologic profiles of coronary atherosclerosis by myocardial bridge underlying myocardial infarction. Atherosclerosis 2013; 226: 118-123.
148. Montecucco F, et al. Systemic and intraplaque mediators of inflammation are increased in patients symptomatic for ischaemic stroke. Stroke 2010; 41: 1394-1404.
149. Davies MJ, et al. Risk of thrombosis in human atherosclerotic plaques: role of extracellularlipid, macrophage, and smooth muscle cell content. Br Heart J 1993; 69: 377-381.
150. Felton CV, et al. Relation of plaque lipid composition and morphology to the stability of human aortic plaques. Arterioscler Thromb Vasc Biol 1997; 17: 1337-1345.
151. Virmani R, et al. Lessons from sudden coronary death: a comprehensive morphological classification scheme for atherosclerosis lesions. Arterioscler Thromb Vasc Biol 2000; 20: 1262-1275.
152. Rodriguez-Granillo GA, et al. In vivo intravascular ultrasound-derived thin-cap fibroatheroma detection using ultrasound radiofrequency data analysis. J Am Coll Cardiol 2005; 46: 2038-2042.
153. Burke AP, et al. Coronary risk factors and plaque morphology in men with coronary disease who died suddenly. N Engl J Med 1997; 336: 1276-1282.
154. Nair ACD, Vince DG. Regularized autoregressive analysis of intravascular ultrasound data: improvement in spatial accuracy of plaque tissue maps. IEEE Trans Ultrason Ferroelectr Freq Control 2004; 51: 420-431.
155. Tian J, et al. Effect of statin therapy on the progression of coronary atherosclerosis. BMC Cardiovasc Disord 2012; 1; 12: 70.
156. de Korte CL, et al. Characterisation of plaque components with intravascular ultrasound elastography in human femoral and coronary arteries in vitro. Circulation 2000; 102: 617-623.
157. Richarda MS, Doyley MM. Investigating the impact of spiral priors on the performance of model-based IVUS elastography. Phys Med Biol 2011; 56: 7223-7246.
158. Liang Y, et al. Measurement od 3D arterial wall strain tensor using intravascular B-mode ultrasound images: a feasibility study. Phys Med Biol 2010; 55: 6377-6394.
159. Burke AP, et al. Coronary calcification: insights from sudden coronary death victims. Z Kardiol 2000; 89: 49-53.
160. Rasheed Q, et al. Correlation of intracoronary ultrasound plaque characteristics in atherosclerotic coronary artery disease patients with clinical variables. Am J Cardiol 1994; 73: 753-758.
161. Nakamura M, et al. Impact of coronary artery remodelling on clinical presentation of coronary artery disease: an intravascular ultrasound study. J Am Coll Cardiol 2001; 37: 63-69.
162. Fujii K, et al. Intravascular Ultrasound Study of Patterns of Calcium in Ruptured Coronary Plaques. Am J Cardiol 2005; 96: 352-357.
163. Lee JB, et al. Histopathologic Validation of the Intravascular Ultrasound Diagnosis of Calcified Coronary Artery Nodules. Am J Cardiol 2011; 108: 1547-1551.
164. Virmani R, et al. Lessons from sudden coronary death: a comprehensive morphological classification scheme for atherosclerotic lesions. Arterioscler Thromb Vasc Biol 2000; 20: 1262-1275.
165. Nishioka T, et al. Contribution of inadequate compensatory enlargement to development of human coronary artery stenosis: an in vivo intravascular ultrasound study. J Am Coll Cardiol 1996; 27: 1571-1576.
166. Mintz GS, et al. Contribution of inadequate arterial remodelling to the development of focal coronary artery stenosis: an intravascular ultrasound study. Circulation 1997; 95: 1791-1798.
167. Birnbaum Y, et al. Regional remodelling of atherosclerotic srteries: a major determinant of clinical manifestations of disease. J Am Coll Cardiol 1997; 30: 1149-1164.
168. Mintz GS, et al. Arterial remodelling after coronary angioplasty: a serial intravascular ultrasound study. Circulation 1996; 94: 35-43.
169. Kimura T, et al. Remodelling of human coronary arteries undergoing coronary angioplasty or atherectomy. Circulation 1997; 96: 475-483.
170. Hartmann M, et al. Relation between baseline plaque burden and subsequent remodelling of atherosclerotic left main coronary arteries: a serial intravascular ultrasound study with long-term (> or = 12 months) follow-up. Eur Heart J 2006; 27: 1778-1784.
171. von Birgelen C, et al. Remodelling index compared to actual vascular remodelling in atherosclerotic left main coronary arteries as assessed with long-term (> or = 12 months) serial vascular ultrasound. J Am Coll Cardiol 2006; 47: 1363-1368.
172. Hong YJ, et al. Positive remodelling is associated with vulnerable coronary plaque commponents regrdless of clinical presentation: Virtual histology-intravascular ultrasound analysis. Int J Cardiol 2012; epub ahead of print.
173. Moreno PR. Vulnerable Plaque: Definition, Diagnosis, and Treatment. Cardiol Clin 2010; 28: 1-30.

174. Barger AC, et al. Vasa vasorum and neovascularisation of human coronary arteries - a possible role in the pathophysiology of atherosclerosis. N Engl J Med 1984; 310: 175-177.
175. Depre C, et al. Neovascularisation in human coronary atherosclerotic lesions. Cathet Cardiovasc Design 1996; 39: 215-220.
176. Ritman EL, Lerman A. Role of vasa vasorum in arterial disease: a re-emerging factor. Curr Cardiol Rev 2007; 3: 43-55.
177. Vavuranakis M, et al. A new method for assessment of plaque vulnerability based on vasa vasorum imaging, by using contrast-enhanced intravascular ultrasound and differential image analysis. Intern J Cardiol 2008; 130: 23-29.
178. Carlier S, et al. Vasa vasorum imaging: a new window to the clinical detection of vulnerable atherosclerotic plaques. Curr Atheroscler Rep 2005; 7: 164-169.
179. O'Malley SM, et al. Intravascular ultrasound based imaging of vasa vasorum for the detection of vulnerable atherosclerotic plaque. Proc. Int Conf Med Image Comput Assist Intery 2005; 8: 343-351.
180. Vavuranakis M, et al. Detection of luminal - intimal border and coronary wall enhancement in intravascular ultrasound imaging after injection of microbubbles and simultaneous sonication with transthoracic echocardiography. Circulation 2005; 112: e1-2.
181. Maresca D, et al. Contrast-enhanced ntravascular ultrasound 3D reconstruction of a vasa vasorum mimicking model. In: Proceedings IEEE Int Ultrasonics Symp, San Diego, CA, USA, 11-14 October 2010.
182. Kume T, et al. Assessment of coronary intima—media thickness by optical coherence tomography: comparison with intravascular ultrasound. Circ J, 2005; 69: 903-907.
183. Prati F, et al. Expert review document on methodology, terminology, and clinical applications of optical coherence tomography: physical principles, methodology of image acquisition, and clinical application for assessment of coronary arteries and atherosclerosis. Eur Heart J 2010; 31: 401-415.
184. Kitabata H, et al. Relation of microchannel structure identified by optical coherence tomography to plaque vulnerability in patients with coronary artery disease. Am J Cardiol 2010; 105: 1673-1678.
185. Vorpahl M, et al. Small black holes in optical frequency domain imaging matches intravascular neoangiogenesis formation in histology. Eur Heart J 2010; 31: 1889.
186. Uemura S, et al. Thin-cap fibroatheroma and microchannel findings in optical coherence tomography correlate with subsequent progression of coronary atheromatous plaques. Eur Heart J 2012; 33: 78-85.
187. Virmani R, et al. Lessons from sudden coronary death: a comprehensive morphological classification scheme for atherosclerotic lesions. Atherioscler Thromb Vasc Biol 2000; 20: 1262-1275.
188. Burke AP, et al. Coronary risk factors and plaque morphology in men with coronary disease who died suddenly. N Eng J Med 1997; 336: 1276-1282.
189. Jang IK, et al. In vivo characterisation of coronary atherosclerotic plaque by use of optical coherence tomography. Circulation 2005; 111: 1551-1555.
190. Kume T, et al. Measurement of the thickness of the fibrous cap by optical coherence tomography. Am Heart J 2006; 152: e1-e4.
191. Sawada T, et al. Feasibility of combined use of intravascular ultrasound radiofrequency data analysis and optical coherence tomography for detecting thin-cap fibroatheroma. Eur Heart J 2008; 29: 1136-1146.
192. Yonetsu T, et al. In vivo critical fibrous cap thickness for rupture-prone coronary plaques assessed by optical coherence tomography. Eur Heart J 2011; 32: 1251-1259.
193. Wang Z, et al. Volumetric quantification of fibrous caps using intravascular optical coherence tomography. Biomed Opt Express 2012; 3: 1413–1426.
194. Tearney GJ, et al. Quantification of macrophage content in atherosclerotic plaques by optical coherence tomography. Circulation 2003; 107: 113-119.
195. MacNeill BD, et al. Focal and multifocal plaque macrophage distributions in patients with acute and stable presentations of coronary artery diseas. J Am Coll Cardiol 2004; 44; 972-979.
196. Kato K, et al. Nonculprit plaques in patients with acute coronary syndromes have more vulnerable features compared with those with non-acute coronary syndromes. Cardiovasc Imaging 2012; 5: 433-440.
197. Yabushita H, et al. Characterisation of human atherosclerosis by optical coherence tomography. Circulation 2002; 106: 1640-16445.
198. Manfrini O, et al. Sources of error and interpretation of plaque morphology by optical coherence tomography. Am J Cardiol 2006; 98: 156-159.
199. Mintz GS, et al. Patterns of calcification in coronary artery disease. A statistical analysis of intravascular ultrasound and coronary angiography in 1155 lesions. Circulation 1995; 91: 1959-1965.
200. Callister TQ, et al. Coronary artery disease: improved reproducibility of calcium scoring with an electron beam CT volumetric method. Radiology 1998; 208: 807-814.
201. Tanigawa J, et al. Heavily calcified coronary lesions preclude stent apposition despite high pressure balloon dilatation and rotational atherectomy: in vivo demonstration with optical coherence tomography. Circ J 2008; 72: 157-160.
202. Tanimoto T, et al. Various types of plaque disruption in culprit coronary artery visualized by optical coherence tomography in a patient with unstable angina. Circ J 2009; 73: 187-189.
203. Stefano GT, et al. Utilisation of frequency domain optical coherence tomography and fractional flow reserve to assess intermediate coronary artery stenoses: conciliating anatomic and physiologic information. Int J Cardiovasc Imaging 2011; 27: 299–308.
204. Kubo T, et al. Assessment of culprit lesion morphology in acute myocardial infarction: ability of optical coherence tomography compared with intravascular ultrasound and coronary angioscopy. J Am Coll Cardiol 2007; 50: 933-939.
205. Chen BX, et al. Characterisation of atherosclerotic plaque in patients with unstable angina pectoris and stable angina pectoris by optical coherence tomography. Zhonghua Xin Xue Guan Bing Za Zhi. 2009; 37: 422-425.
206. Mizukoshi M, et al. Clinical classification and plaque morphology determined by optical coherence tomography in unstable angina pectoris. Am J Cardiol 2010; 106: 323-328.
207. Jang IK, et al. Visualisation of coronary atherosclerotic plaques in patient using optical coherence tomography: comparison with intravascular ultrasound. J Am Cardiol 2002; 39: 604-609.
208. Meng L, et al. In vio optical coherence tomography of experimental thrombosis in a rabbit carotid model. Heart 2008; 94: 777-780.
209. Bezerra HG, et al. Intracoronary optical coherence tomography: a comprehensive review clinical and research applications. JACC Cardiovasc Interv 2009; 2: 1035-1046.
210. Kume T, et al. Relationship between coronary remodelling and plaque characterisation in patients without clinical evidence of coronary artery disease. Atherosclerosis 2008; 197: 799–805.
211. Raffel OC, et al. In vivo association between positive coronary artery remodelling and coronary plaque characteristics assessed by intravascular optical coherence tomography. Eur Heart J 2008; 29: 1721–1728.
212. Rathore S, et al. Association of coronary plaque composition and arterial remodelling: A optical coherence tomography study. Atherosclerosis 2012; 221: 405–415.
213. Kubo T, et al. Virtual histology intravascular ultrasound compared with optical coherence tomography for identifcation of thin-cap fibroatheroma. Int Heart J 2011; 52: 175-179.
214. Kubo T, Akasaka T. OCT-ready for prime time? Clinical applications of optical coherence tomography. Cardiac Interv Today 2009; 4: 35-37.
215. Takarada S, et al. Advantage of next generation frequency-domain optical coherence tomography compared with conventional time-domain system in the assessment of coronary lesions. Catheter and Cardiovasc Interv 2010; 75: 202-206.
216. Kubo T, Akasaka T. Optical coherence tomography imaging: current status and future perspectives- current and future developments in OCT. Cardiovasc Interv Therap 2009; 25: 2-10.
217. Tearney GJ, et al. Optical coherence tomography for imaging in the vulnerable plaque. J Biomed Opt 2006; 11: 021002.
218. Tearney GJ, et al. Three-dimensional coronary artery microscopy by intracoronary optical frequency domain imaging. JACC: Cardiovasc Imag 2008; 1: 752-761.
219. Gao D, et al. Computed tomography for detecting coronary artery plaques: a meta-analysis. Atherosclerosis 2011; 219: 603-609.
220. Deliargyris EN. Intravascular ultrasound virtual histology derived thin cap fibroatheroma: now you see it, now you don't. J Am Coll Cardiol 2010; 55: 1598-1599.
221. Nahrendorf M, et al. Noninvasive vascular cell adhesion molecule-1 imaging identifies inflammatory activation of cells in atherosclerosis. Circulation 2006, 114: 1504–1511.